UNIVERSITÉ DE SHERBROOKE

Faculté de génie

Département de génie mécanique

MÉCANIQUE ET MÉCANISME DE PERFORATION DES MATÉRIAUX DE PROTECTION

Thèse de doctorat en génie (SCA 799)

Directeur de recherche :

Toan VU-KHANH

C. Thang NGUYEN

Sherbrooke (Québec), Canada Juillet 2009

Your file Votre référence
ISBN: 978-0-494-52846-4
Our file Notre référence
ISBN: 978-0-494-52846-4

UNIVERSITÉ DE
SHERBROOKE

Faculté de génie

Département de génie mécanique

MECHANICS AND MECHANISM OF PUNCTURE OF PROTECTIVE MATERIALS

Doctoral thesis in applied science (SCA 799)

Director of research :

Toan VU-KHANH

C. Thang NGUYEN

Sherbrooke (Québec), Canada July 2009

RÉSUMÉ

La résistance à la perforation fait souvent partie des propriétés mécaniques les plus importantes pour les vêtements de protection, en particulier dans le secteur médical. Cependant, les paramètres intrinsèques du matériau qui contrôlent la résistance à la perforation des matériaux de protection sont encore inconnus. L'objectif de ce travail est donc d'étudier le mécanisme de perforation et les comportements mécaniques des vêtements de protection lorsqu'ils sont soumis à divers types de sondes de perforation. Une meilleure compréhension de la mécanique de la perforation permettra de développer des méthodes appropriées pour évaluer la résistance à la perforation des matériaux des vêtements de protection et prédire leur rupture.

Cette thèse comprend quatre articles qui décrivent les deux aspects principaux de cette étude. Les articles I et II présentent la mécanique et les mécanismes de perforation par les sondes coniques et cylindriques utilisées dans les méthodes d'essai normalisées (ASTM F1342 et ISO 13996). Les résultats montrent que la perforation des membranes élastomères par des sondes coniques et cylindriques est contrôlée par une déformation locale maximale (ou déformation à la rupture en perforation) qui est indépendante de la géométrie de la sonde. Les valeurs de résistance en perforation des membranes élastomères sont beaucoup plus faibles que celles en tension et en déformation biaxiale. De plus, il a été montré qu'une sonde cylindrique plus simple peut être utilisée à la place de la sonde conique coûteuse de la méthode ASTM, pour fournir une caractérisation quantitative de perforation. De fait, depuis 2005, une méthode alternative B avec une sonde cylindrique de 0,5 mm de diamètre à extrémité arrondie a été ajoutée au texte de la norme ASTM F1342.

D'autre part, les sondes de perforation utilisées dans la norme ASTM F1342 sont très différentes des objets pointus réels (aiguille médicale, pointe de couteau...) et ne peuvent pas caractériser de manière exacte la résistance à la piqûre par de vrais objets. Par conséquent, dans une seconde étape, la mécanique et les mécanismes de piqûre par les aiguilles médicales ont été étudiés. L'article III montre que la piqûre par des objets à pointe coupante tels que les aiguilles médicales est très différente de la perforation par les sondes coniques utilisées dans la norme ASTM F1342. Pour les aiguilles médicales, la résistance à la piqûre implique le phénomène de coupure et l'énergie de rupture du matériau. En utilisant la mécanique de la

rupture, l'énergie de rupture en perforation a été évaluée à partir de la variation de l'énergie de déformation créée par une modification de la surface de la fissure. Ce calcul suppose qu'il n'y a pas de friction entre la pointe de l'aiguille et la surface de la fissure. Cependant, même avec l'application d'un lubrifiant sur la surface de l'aiguille, l'effet de la friction sur le processus de piqûre ne peut pas être complètement éliminé, ce qui empêche la détermination de l'énergie de rupture du matériau. Par conséquent, l'article IV décrit une méthode, similaire à celle de Lake et Yeoh pour la coupure, développée pour évaluer la valeur exacte de l'énergie de rupture de piqûre des caoutchoucs par des objets à pointe coupante. La méthode permet d'éliminer substantiellement les effets de la friction lors de l'évaluation de l'énergie de rupture impliquée dans le processus de la piqûre.

Mots-clés

Perforation, piqûre, élastomère, aiguille médicale, friction, énergie de rupture, sonde conique

SUMMARY

Puncture resistance is among the major mechanical properties often required for protective clothing, especially in the medical sector. However the intrinsic material parameters controlling puncture resistance of protective materials are still unknown. Therefore, the purpose of this work is to study the mechanism and mechanical behaviors of puncture resistance of protective clothing materials to various probe types. A better understanding of puncture mechanics will be helpful to develop suitable methods to evaluate the puncture resistance and to predict the failure of protective clothing materials.

The thesis includes 4 articles which expose two major phases in this study. *Article I and II* studied the mechanics and mechanisms of puncture by conical and cylindrical probes used in the standard test methods (ASTM F1342 and ISO 13996). The results show that the punctures of rubber membranes by conical and cylindrical probes are controlled by a maximum local deformation (or puncture failure strain) that is independent of the probe geometry. The puncture strengths of elastomer membranes are much lower than their tensile and biaxial strengths. In addition, a simpler cylindrical probe can be used in the place of the costly conical probe required by the ASTM standard and still provides a quantitative characterization of puncture. Actually, since 2005, an alternative method B had been added to F1342 ASTM with 0.5 mm-diameter rounded-tip cylindrical probe.

Furthermore, the puncture probes used in the ASTM F1342 are very different to the actual pointed objects (*medical needle, pointed tip of knife...*) and cannot accurately characterize the puncture resistance to real objects. Therefore, in the second step, the mechanics and mechanisms of puncture by medical needles were studied. *Article III* shows that the puncture by sharp-pointed objects like medical needles is very different from the puncture by conical probes used in the ASTM standard test. For medical needles, the puncture resistance involves cutting and fracture energy of material. Using the fracture mechanics, based on the change in strain energy with the change in fracture surface, the fracture energy in puncture was estimated. This calculation assumes that there is no friction between the needle tip and fracture surface. However, even with the application of a lubricant on the needle surface, the effect of friction on the puncture process cannot be totally eliminated, preventing

the determination of the material fracture energy. Therefore, *Article IV* has described a method, similar to that of Lake and Yeoh for cutting to access the precise value of fracture energy in puncture of rubbers by sharp-pointed objects. The method allows substantially eliminating the effects of friction on the evaluation of the fracture energy involved in the puncture process.

Keywords

Puncture, elastomer, medical needle, friction, fracture energy, conical probe

ACKNOWLEDGMENTS

I would like to thank my director of research, Professor Toan Vu-Khanh, for his guidance, helpful discussions and editing of all articles. I wish to thank him again for the financial support, which allowed me to follow the studying program.

I would like to thank the Ecole de Technologie Supérieure. My thanks especially go to Dr. Patricia Dolez who edited the articles III & IV with Prof. Vu-Khanh and helped me a lot in this thesis.

I wish to thank the Institut de Recherche en Santé et en Sécurité du Travail du Québec (IRSST) for the support of this study. My thanks particularly go to Dr. Jaime Lara, Department of Security Engineering, IRSST for the valuable advice and help.

TABLE OF CONTENTS

LIST OF FIGURES

LIST OF TABLES

NOMENCLATURE

A	Area of the fracture surface (mm^2)
a_T	Shift factor
C	Cutting energy (J/m^2)
C_1, C_2	Mooney-Rivlin coefficients
c	Cut length (mm)
d	Crack tip diameter (mm)
E	Tensile modulus (Mpa)
E_a	Activation energy (kJ/mol)
F	Applied force (N)
G, G_c	Fracture energy, tearing energy (J/m^2)
G_o	Threshold energy (J/m^2)
λ	Extension ratio
R	Gas constant (J/mol/K)
R_T, R_{Tg}	Equivalent rates at temperatures T and T_g
σ	Engineering stress (Mpa)
σ^{true}	True stress (Mpa)
e	Engineering strain (%)
ε	True strain (%)
T	Tearing energy (J/m^2) or absolute temperature (^oK)
T_s, T_{ref}	Reference temperature (^oK)
T_g	Glass transition temperature (^oK)
T_c	Critical tearing energy (J/m^2)
U	Total elastic energy (J)
W	Strain energy density (J/m^3)
W_t	Strain energy density at the crack tip (J/m^3)
LEFM	Linear Elastic Fracture Mechanics
ASTM	American Society for Testing and Materials
IRSST	Institut de Recherche en Santé et en Sécurité du Travail du Québec
ÉTS	École de Technologie Supérieure, membre du réseau de l'Université du Québec

CHAPTER 1

INTRODUCTION

Puncture resistance of protective materials has been an important issue for a long time in many fields. Especially in the medical sector, health care workers may be infected with viruses, diseases, or infectious substances through punctured holes on protective equipment. In the United States, according to the Occupational Safety and Health Administration (OSHA) estimates, more than 5.6 million workers in health care and public safety occupations could be exposed to the human immunodeficiency virus (HIV) and the Hepatitis B virus (HBV). The most common type of percutaneous injury was an inadvertent needlestick injury. And overall, protective equipment prevented 87% of all skin and face contact [1].

Puncture resistance is among the major mechanical properties of protective gloves made of elastomer membranes, yet the intrinsic material parameters controlling the puncture resistance of these materials are still unknown. Various investigations have been performed on specific cases involving different materials. However, the reported investigations are either qualitative, and do not provide a fundamental understanding of the mechanisms controlling puncture, or are not applicable to the highly elastic elastomer membranes. The following section outlines the reported works on puncture involving different behaviours in various materials.

The puncture resistance of protective gloves to surgical needle was studied in [1]. In this work, 19 commercially available surgical glove liners were ranked according to a measurement of the puncture force. The resistance of finger guards, glove liners and thicker latex gloves to needle penetration were also measured in order to compare these materials in terms of puncture protection with respect to the single latex glove [2]. The effectiveness of cut-proof glove liners on cut and puncture resistance, dexterity, and sensibility are discussed in [3]. However, the thickness is not taken into account in these works, and the results are only qualitative for purposes of comparison. More fundamental investigations on puncture have been carried out on rubber blocks by fracture mechanics [4]. With a cylindrical indentor, it was has been shown that a starter crack initiates as a ring on the rubber-block surface before

puncture occurs. Using fracture mechanics, a method has been developed to calculate the fracture energy in puncture. The puncture energy values obtained were found to agree with the catastrophic tearing energy obtained from trouser tear tests. However, the rubber-block situation involves surface indentation and is not applicable to the case of puncture of elastomer membranes. The quantitative characterization of puncture resistance has also been developed for geotextiles and geomembranes. In these materials, a correlation was found between the puncture force and the tensile strength for probes greater than 20 mm in diameter [5-7]. Considering a loading state of pure axisymmetric tension, the puncture resistance of geotextile membranes was calculated in term of tensile wide-width strength. To simulate the actual application in service, the puncture of pre-strained geotextiles was also analyzed in [8] and the relationship between puncture resistance and tensile wide-width strength was confirmed. However, the results are only applicable in the case of linearly elastic deformation. Thin rubber membranes, for their part, are hyperelastic and highly nonlinear.

Presently, to evaluate puncture resistance of protective clothing, the standard tests ASTM F1342 and ISO 13996 are the most commonly used methods. These tests have been developed to evaluate the puncture resistance of thin flexible-materials. The ASTM F1342 [9] is designed for any type of protective clothing, including coated fabrics, laminates, textiles, plastics, elastomeric films or flexible materials. This test method determines the puncture resistance of a material specimen by measuring the maximum force required for a conical puncture probe to penetrate through a specimen clamped between two plates with chamfered holes of diameter less than 10 mm. However, this method is only qualitative characterization and does not provide the intrinsic material properties that control puncture resistance.

Furthermore, it is clear that the puncture probe used in the ASTM F1342 (Figure 1.1) is very different to the actual pointed objects (Figure 1.2) and cannot accurately characterize the puncture resistance to real objects. In fact, puncture of protective clothing materials by

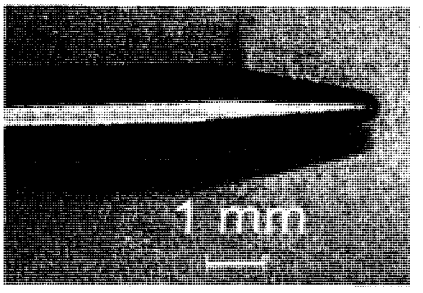

Figure 1.1: Puncture probe used in ASTM F1342

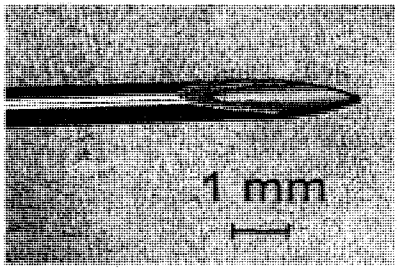

a) Medical needle

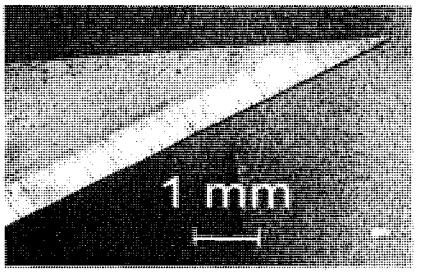

b) Pointed tip of a knife

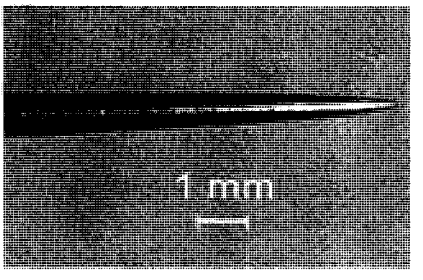

c) Sewing needle

Figure 1.2: Actual pointed objects.

medical needles (Figure 1.2a) has been studied [1-3] and the puncture resistances are found much smaller than those measured by the ASTM F1342. In addition, in these works, the thickness is not taken into account hence thicker samples give higher resistance and the intrinsic material parameter controlling puncture resistance is still unknown. Therefore, additional studies should be carried out on the puncture probes which are similar to real objects (e.g. medical needles can be used as puncture probes) and new testing methods should be developed for a more realistic characterization of the puncture resistance of protective clothing materials.

In terms of fracture mechanics, puncture caused by sharp objects (Figure 1.2a & 1.2b) is a complex phenomenon and may involve the combination of puncture and cut (or tear) that may happen simultaneously. In fact, there are few protective materials that can resist multiple risks (puncture and cut simultaneously). The studies carried out by IRSST (Institut de recherche Robert-Sauvé en santé et en sécurité du travail du Québec) demonstrated that in almost cases, protective materials have very high cut resistance, but low puncture resistance and vice-versa [10 - 12]. Recently, the development of a method to study the combined puncture and tear of fabrics has been carried out [13]. However, this experimental method is still in the primary stage of development and the obtained results only show the parameters of the apparatus that affect the tear propagation of woven fabrics.

Therefore, the purpose of this work is to study the mechanism and mechanical behaviors of puncture resistance of protective clothing materials to various probe types. The environmental effects on puncture performance, such as temperature, loading rate and physical aging effects will be also investigated. A better understanding of puncture mechanics will be helpful to develop suitable methods to evaluate puncture resistance and to predict the failure of protective clothing materials as well as to develop new protective materials for better puncture resistance.

CHAPTER 2

REVIEW OF THE LITERATURE

2.1 Materials for protective clothing

Common materials for protective clothing are rubbers, flexible thermoplastics and polymer fabrics as listed in Table 2.1 [14].

TABLE 2.1: COMMON MATERIALS FOR PROTECTIVE CLOTHING [14]

Material name	Other material names
Butyl	I I R (rubber)
Natural rubber	N R (rubber)
Neoprene	Polychloroprene rubber or CR
Nitrile	Acrylo-nitrile butadiene rubber or NBR
Hypalon (^{TM})	Chlorosulphonated ethylene rubber
Viton (^{TM})	Fluorocarbon rubber or FPM
PE	Polyethylene
PVC	Polyvinyl chloride
PVA	Polyvinyl alcohol
CPE	Chlorinated polyethylene
EVOH	Ethylene-vinyl alcohol
Saranex (^{TM})	PE/Polyvinylidene chloride or PE/Saran
Teflon (^{TM})	Polytetrafluoroethylene (TFE or PTFE)
Kevlar (^{TM}) & Nomex (^{TM})	Polyaromatic amide
UHMWPE	Ultra-high molecular weight polyethylene

(^{TM}) = Trademark

Various polymer materials mentioned above have different mechanical properties. The typical tensile stress-strain curves for different polymers are shown in Figure 2.1 [15]. In the case of fibber (polymer fabric), deformation is elastic up to brittle failure point with high tensile modulus, low extension at break and high breaking stress (curve 2). Flexible plastic has a lower modulus but it is capable of undergoing yield and extensive plastic deformation (curve 3). Rubbers have relatively low values of Young's modulus and are capable of extending reversibly up to over 500% before eventual failure (curve 4).

The polymers are also viscoelastic materials that exhibit a combination of elastic and viscous behavior. As known, viscoelasticity behavior is especially prominent in polymers with the result that the mechanical properties strongly depend on the time and temperature. Mechanical properties of polymers also depend on the molecular structure, the molecular weight, and mechanical processing such as roll, draw, and extrude.

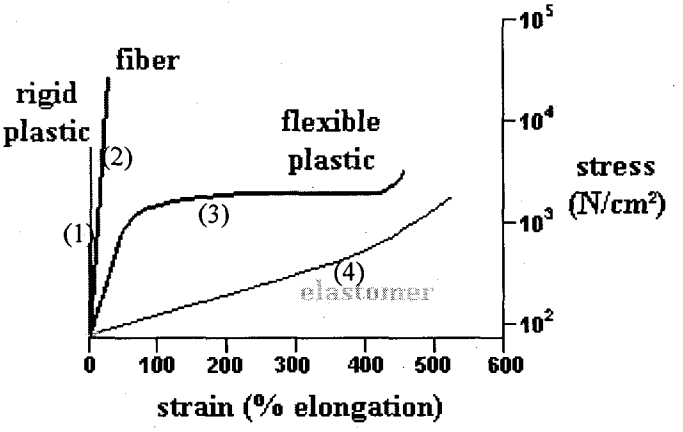

Figure 2.1: Sketch of stress-strain curves for various types of polymer [15].

Some thermoplastics with good chemical-resistance (PVA) and water-resistance (PVC, PP, PE...) are used for protective clothing (Table 2.1). Unfortunately, these materials are either uncomfortable to wear, lack good tactility, are fragile or expensive. For example, polyvinyl alcohol (PVA) polymer offers excellent resistance against many organic substances but is highly sensitive to degradation by water and ineffective for extended use where perspiration occurs [14]. Thus, a rubber such as natural rubber, neoprene, nitrile, or butyl rubber is employed alternatively.

Rubber membranes are widely used for medical gloves and protective clothing due to their hyperelastic properties, leading to high flexibility and sensibility for operators. Most materials obey the Hooke's law under small elastic deformation whereas rubber has a hyperelasticity and a highly non-linear behavior. In this case, the Hooke's law cannot be applied and the non-linear Mooney-Rivlin equation is appropriate for rubber's deformation [16 - 20].

Rubbers have hyperelastic behavior, good water and oil resistance, but low strengths, low cut and tear resistance. Fibers have very high strength and some fibers like Kevlar can withstand high temperature. However fibbers have low extension, weak resilience and do not have capacity of water or oil resistance. Fiber fabrics and rubber are combined to obtain a fiber-reinforced composite that has the properties of both components: flexibility, water-resistance, high strength and/or withstand high temperature.

Common commercial composite materials used to make protective clothing are: woven cotton fabric, or woven spectra fabric, or woven kevlar fabric embedded in polyisoprene, neoprene or nitrile. Many composite structures have been developed for a better cut and/or puncture resistance material. For example, Gimbel Gloves have developed a multilayers composite pad for better puncture resistance on the fingertips. The protective pads are made from an innovative weaving process. Nine layers of puncture-resistant polymer mesh are sealed around the edges so each layer moves independently (Fig. 2.2). The pads are sealed between two layers of latex providing maximum protection while maintaining manual dexterity and tactile feel. These pads have 1800% more puncture-resistance than double gloving with standard latex gloves (http://www.cfrd.org).

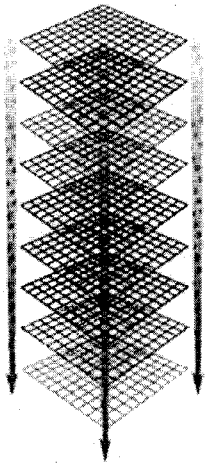

Figure 2.2: Puncture-resistant polymer mesh in Gimbel Gloves.

2.2 Fracture mechanics of polymers

Puncture, cutting, tearing are different kinds of failure in polymers that involve fracture mechanics. During the deformation and fracture of polymers, the molecules slide past each other and tend to uncoil, breaking secondary bonds. Molecular fracture through the scission of primary bonds will take place if the flow of molecules passing each other is restricted due to the nature of polymer structure such as in a semi-crystalline polymer, in cross-linked polymer, in polymer fibbers etc. There are many general approaches to the study of fracture in polymers.

2.2.1 Theoretical strength

Fracture involves the creation of new surfaces in a body, and in polymer that occurs by the breaking of primary (covalent) and/or secondary (e.g., van der Waals or hydrogen) bonds. An estimate of the theoretical strength of a solid polymer can be made by the simple analysis of Kelly and MacMillan [21, 22] developed for any type of solid. When different values of E (Young's modulus of the material), G_0 (the energy required to create new surfaces) and a_0 (the equilibrium separation of the interatomic planes perpendicular to the tensile axis) are put into the above estimate, it is found for most solids that the maximum tensile strength can be approximated by [21, 22]:

$$\sigma_{th} \approx E/10 \qquad (2.1)$$

The interest of the 'theoretical strength', σ_{th}, is that it gives the upper limit of strength expected for the materials. However, the measured values of tensile strength σ_f are about E/100 – E/30 for most materials because of the presence of flaws acting as stress concentrators [21, 22].

2.2.2 Fracture mechanics

It was shown in the previous section that the theoretical strength of a solid is of the order of E/10. However, the measured strengths are often well below the theoretical value.

Griffith showed that the relatively low strength of a brittle solid could be explained by the presence of flaws acting as stress concentrators [23]. This hypothesis has been developed and extended by many investigators and is the basic of "fracture mechanics" which is used to interpret the fracture of many solids, including polymers.

Two main approaches are used in fracture mechanics although they are closely related. The first is an energy criterion developed by Orowan which supposes that fracture takes place when sufficient energy is released during crack growth to supply the energy of the new fracture surfaces created [22]. The fracture of a material is thereby characterized by the material property G_c known as the 'strain energy release rate' or 'fracture energy':

$$-\left(\frac{\partial W}{\partial A}\right)_l = G_c \qquad (2.2)$$

where W is the total elastic energy in the sample considered and A the area of one fracture surface of the crack. The partial derivative indicates that the sample considered is held at constant length l, so that the applied forces do not move, hence do no work.

The second approach was developed by Irwin who showed that the stress field around a sharp crack in an elastic material could be uniquely defined by a parameter known as the 'stress intensity factor' K [22]. Fracture then occurs when K reaches a critical value K_c, which is material property often called the 'fracture toughness'. The parameters G_c and K_c are related for a linear elastic material through the approximate relationship:

$$G_c \approx K_c^2/E \qquad (2.3)$$

Another approach based on local analysis around a crack tip was developed by Thomas [24] for elastomer: nonlinear elastic material. If a suitably averaged strain energy density at the tip is U_t and with a model crack having a semicircular tip of diameter d, the approximate relation is:

$$G_c = U_t\, d \qquad (2.4)$$

The confirmation of this relationship by experimental study [24] supports the contention that the region surrounding the crack tip where the local dissipation, arising from hysteresis and bond rupture mechanisms, is the characteristic of the fracture process. And the value of G_c, determined from any particular test method, should be independent of geometrical and loading considerations [20, 22, 25].

2.3 Reported approaches on puncture of various materials

Puncture resistance is among the major mechanical properties in many fields, e.g., the Occupational Safety and Health, the Geotechnical... Various investigations have been performed on specific cases involving different materials. However, the reported investigations are either qualitative and do not provide a fundamental understanding of the mechanisms controlling puncture, or are not applicable to the protective clothing materials. The following sections outline the reported fundamental studies on puncture of various materials.

2.3.1 Puncture of rubber blocks

For rubbers, conventional tensile and tear tests are not particularly suitable tools for investigation of strength-properties of small components (not large enough for tensile and tear tests) or over the thickness of a bulky product. An alternative approach, particularly suitable for diagnostic work, involves the use of a puncture test [4]. A probe of specified geometry is pressed into the component, and the force to cause rupture is measured at specified penetration depths. One suitable application is the study of aging across the thickness of a bulky product [25]. The effects of aging are stronger at the small depth near the surfaces where material contacts with the environment (oxidative agents...).

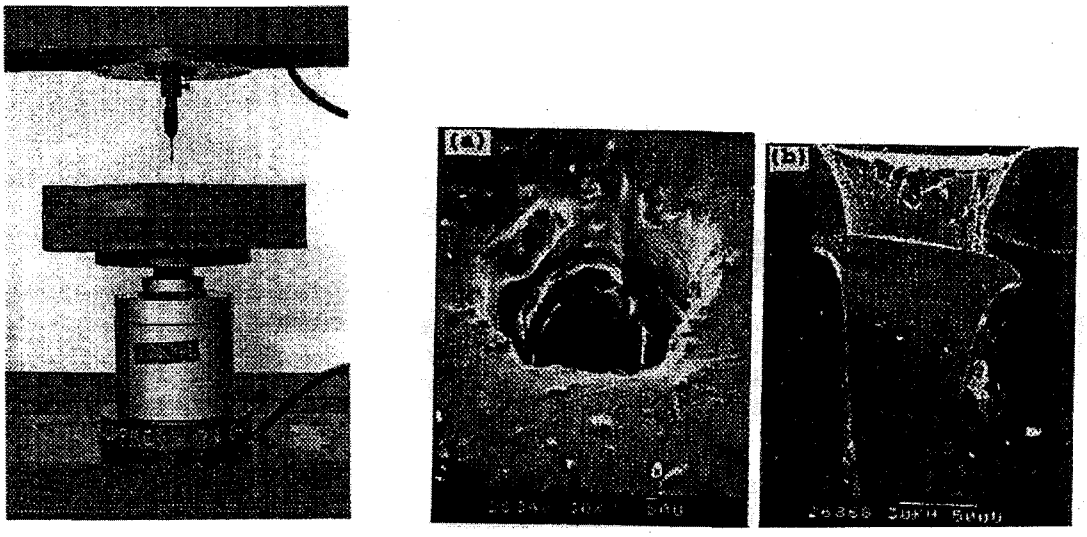

a) Test arrangement b) Top view and section view of ring cracks

Figure 2.3: Puncture testing of rubber blocks [4].

With a sharp cylindrical probe, a starter crack initiates as a ring on the rubber surface before puncture takes place. Using fracture mechanics, an equation has been derived for the energy of puncture. The puncture force F at rupture is related to the tearing energy G_c by the equation:

$$G_c = F\frac{1-\lambda_c}{2\pi r_o} \qquad (2.5)$$

where λ_c is the compression ratio and r_o is the surface crack radius after rupture. Good agreement has been reported between tearing energies derived from the test and those from trouser tear measurements [4].

This approach is for rubber blocks, but it may be useful for the puncture study of rubber membranes. Furthermore, for needle diameters which are very small compared to sample thickness or puncture of rubber sample on the support (simulating protective clothing in wear), the puncture performance may be related to this study of rubber block.

2.3.2 Puncture of geotextiles

For geotextiles and geomembranes in geotechnical applications, there is a sub-domain to study puncture behavior and it has been successfully applied to simulate, design and predict the failures in the real structures [5 - 8].

In designing with geotextiles, there is a need for an assessment of geotextile resistance to objects such as rocks or pieces of wood under quasi-static conditions. Such a test is described as the California bearing ratio (CBR) test [5] (devised by the California State Highway Association). There is a direct relationship between this type of puncture resistance value and the tensile wide-width strength of the geotextile. This is because the geotextile between inner edge of the specimen holder and outer edge of the puncturing rod is indeed in state of pure axi-symmetric tension. Cazzuffi et al. proposed the following empirical equation as a correlation between the breaking force of the CBR test and the wide-width tensile strength for isotropic, nonwoven geotextiles [5, 6]:

$$T_f = F_p / 2\pi r \qquad (2.6)$$

where T_f = the tensile force per unit width of fabric, kN/m, and

F_p = the puncture breaking force, kN

and r = the puncture probe radius, m.

The puncture phenomenon of geomembrane when pierced by objects such as rocks or pieces of wood is different from that of the protective clothing caused by small needles. However, fiber-reinfored composites have the similar structures to geomembranes, therefore the puncture approaches of geomembranes may be helpful for the puncture study of fiber composites used for the protective clothing.

2.3.3 Puncture of protective clothing

Some works on the puncture of protective clothing have been carried out [1-3]. However, most of the reported investigations are qualitative and deal only with measurements

of the forces required to perforate a thin protective material. The puncture behavior and material parameters controlling puncture performance are still unknown.

Presently, to characterize protective materials, standard test methods have been used to evaluate the puncture resistance such as ASTM F1342 and ISO 13996. The ASTM F 1342 [9] is designed for any type of protective clothing, including coated fabrics, laminates, textiles, plastics, elastomeric films or flexible materials. This test method determines the puncture resistance of a material specimen by measuring the force required to cause a puncture probe to penetrate through the specimen (Fig. 2.4). The specimen is fixed between two plates, each plate has three chamfered holes of 6 mm diameter. The open spaces centered below 10 mm guide holes should be enough to allow for 25 mm of travel of the probe (see Fig. 2.4b).

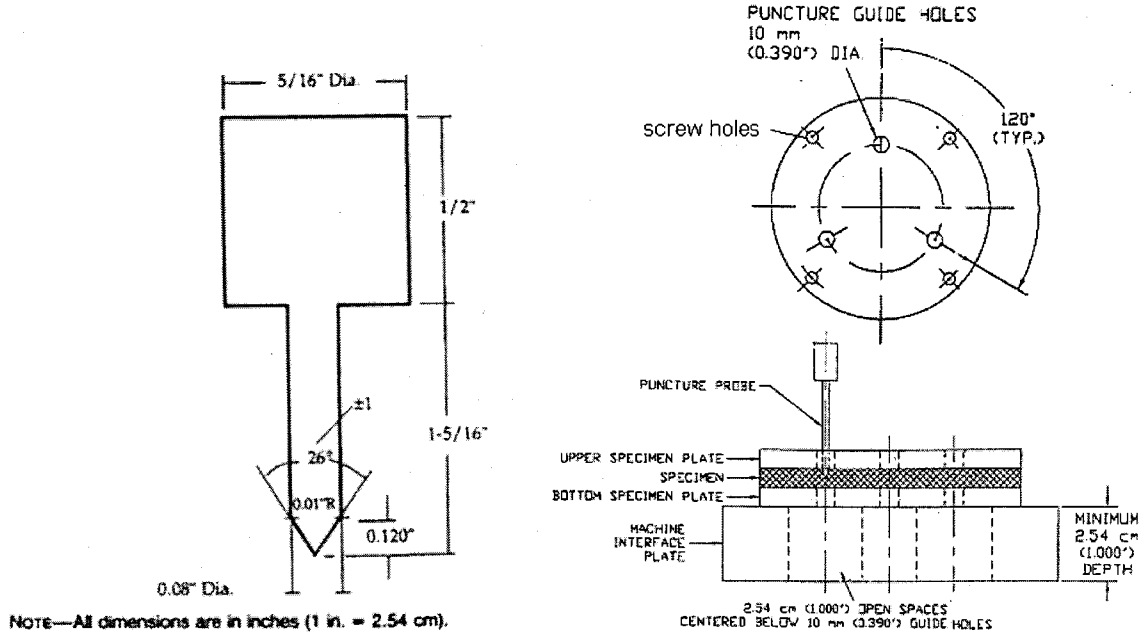

a) Cross-section of puncture probe b) Side view of specimen support

Figure 2.4: Puncture test probe and specimen support of ASTM F1342 [9].

However, this test method is not intended to measure puncture resistance of all types of punctures encountered using protective clothing. For example, with sharp medical needles, the puncture resistance is much lower than that measured by this test method [1]. Furthermore, in the ASTM F1342, the conical probe tip is difficult to reproduce, that lead to

difficulty in reproducing the puncture force by different labs [10]. Therefore, the study of alternative cylindrical probes to evaluate the puncture resistance of protective clothing materials has been carried out at IRSST [10]. In this work, the relations between puncture force and puncture probe velocity, probe diameter were also investigated. However, all above methods do not provide the material parameters controlling puncture performance or governing mechanism that would be used in more general applications.

As mentioned previously, puncture caused by actual sharp and pointed object (medical needle, pointed tip of a knife) is different from that by the conical probe or cylindrical probe in the existing test methods. In the case of sharp and pointed object, puncture is a complex phenomenon and may involve the combination of puncture and cut (or tear) that happens simultaneously. For the determination of combined puncture and tear resistance of flexible materials, the existing method is the ASTM D2582. This test method covers the determination of the dynamic tear resistance of plastic film and thin sheeting subjected to end-use snagging-type hazards (Fig. 2.5). In this method, a probe is dropped by a carriage onto the surface of the test material that is held in a specimen holder at an angle nearly 90^0 to the probe (Fig. 2.5). Samples are individually mounted in a test fixture and held in place by five clamps. A sharp-edged probe is mounted onto a weighted drop mass, which falls along guide rails. This mass is dropped so that the probe comes in contact with the sample, causing it to puncture and tear.

However this method is designed for plastic film and thin sheeting, therefore it is not suitable for the complex variety of protective clothing materials. The development of a method (based on the ASTM D2582) to study the combined puncture and tear of fabrics has been carried out recently [13]. However, the method and the device is still in the primary stage of development, the work was done to understand only the parameters of the apparatus affecting the tear propagation of woven fabrics.

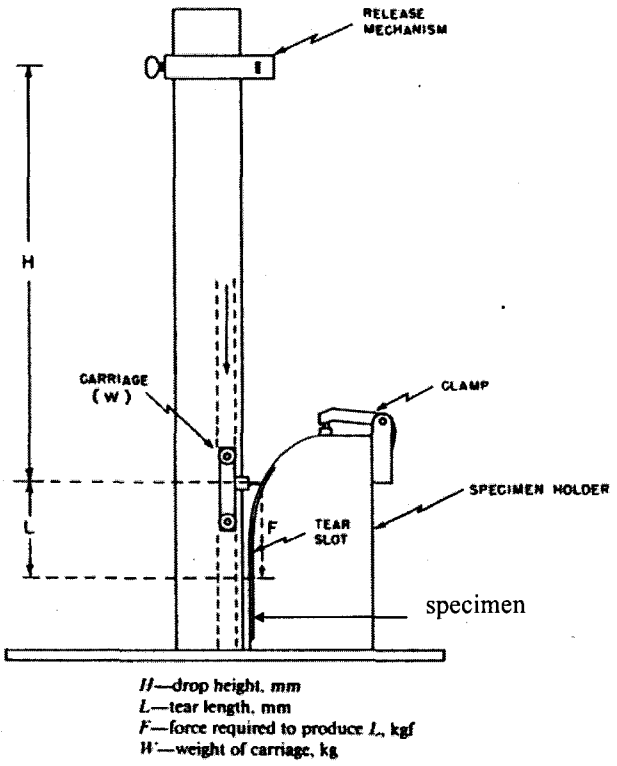

Figure 2.5: Puncture-propagation of tear tester (ASTM D2582).

Therefore, the studies should be carried out on the puncture probes which are similar to real objects (e.g. medical needles can be used as puncture probes) and new testing methods should be developed for a more realistic characterization of the puncture resistance of protective clothing. Also, it is necessary to study the behavior of materials in the combined puncture and cut (or tear) performance (simulating the multiple risks in using of protective clothing).

CHAPTER 3

METHODOLOGY

3.1 Objectives and scope of the study

The purpose of the study is to understand the mechanism and mechanical behaviors of puncture resistance of common protective clothing materials to various puncture probe types, to find the intrinsic material properties that control puncture resistance and to develop an analytical correlation between the puncture resistance and other mechanical properties (such as tensile strength, fracture toughness...). A better understanding of puncture mechanics will be helpful to develop suitable methods to evaluate puncture resistance and to predict the failure of protective clothing materials as well as to develop new protective materials for better puncture resistance.

- The following experimental and analytical methods are used:

(a) The puncture tests of protective materials are carried out using test methods proposed recently (see Section 2.3.3 and 4.1).

(b) Tensile and tear tests on the studied materials are performed according to ASTM D412 and ASTM D624 respectively, for determining the tensile strength and fracture toughness of materials (Section 4.1 and 4.2).

(c) Analyze/determine the criteria (material fundamental parameters) that control the puncture failure and to find an analytical correlation between the puncture resistance and other mechanical properties (such as tensile strength, fracture toughness) based on the above experimental results.

(d) The effects of test parameters (probe geometry, sample holder size, sample thickness...) on puncture resistance are also investigated.

3.2 Choice of materials for the proposed study

Common commercial protective clothing materials used for this study are:

+ Rubbers:

- Neoprene sheets with various thickness and hardness from Fairprene Industrial Products Co., USA,
- Nitrile of various thickness cut from gloves of Ansell Edmont Co., England,
- Natural rubber from gloves of Sandstrahler Co. with various thickness.

+ Fiber-reinforced composites and Flexible plastics:

- Composites of woven Kevlar and rubber (neoprene or nitrile) from Best gloves and Ansell Edmont gloves.
- Puncture tests have been carried out on polyethylene (PE) and composites of Kevlar in this study. However, they are only the preliminary results of effects of testing parameters on the puncture resistance.

CHAPTER 4

EXPERIMENTAL

4.1 Puncture test

The puncture tests are carried out on the same test equipment and procedure developed by Lara et al. [10]. Testing apparatus is showed in Figure 4.1. The sample is held between two steel plates pressurized by air at 0.8 MPa. The hole of the lower plate is chamfered to avoid the stress concentration. Two sizes of the sample holder diameter are available: D_h = 38.0 mm and 13.5 mm.

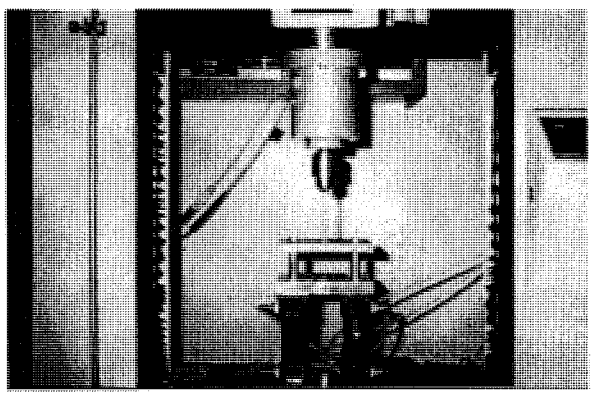

Figure 4.1: a) Puncture test apparatus.

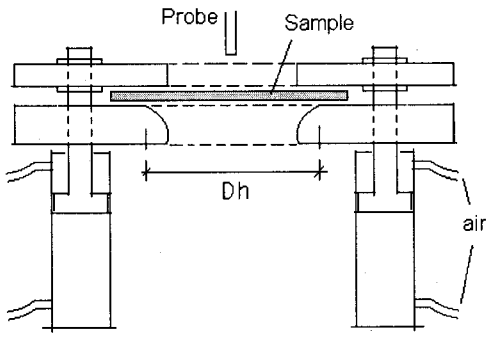

b) Sketch of sample holder.

The puncture probe is clamped in a pin chuck mounted to loadcell in the test machine crosshead (universal-testing machine Instron - Model 1137), which then forced the probe on the sample membrane. The force and the vertical displacement during the test are recorded.

Three types of puncture probe are used: cylindrical probes (flat tip & rounded tip), conical probes (flat tip & rounded tip) and medical needles (Figure 4.2). All probes are made of stainless steel.

For the cylindrical probes, probe diameters of the flat tip (Figure 4.2a) are 0.1 mm, 0.2 mm, 0.5 mm, 1.0 mm, 1.4 mm and 2.5 mm. The diameters of the rounded tip (Figure 4.2b) are 1.0 mm and 2.5 mm.

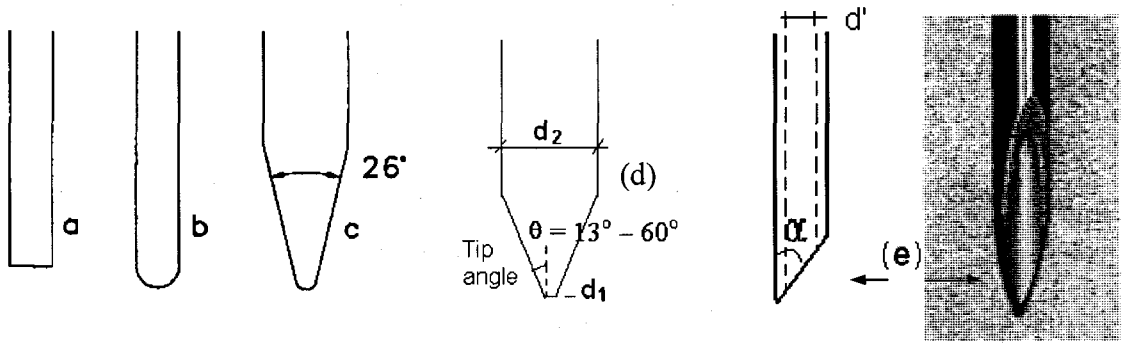

Figure 4.2: Puncture probes: cylindrical probes: flat tip (a), rounded tip (b), conical probes: rounded tip (c), flat tip (d) and medical needle (e).

For the conical probes with rounded tip (Figure 4.2c), the conical extremities have an angle of 26^0 and 3 probe sizes are used whose rounded end have 0.25 mm , 0.30 mm and 0.50 mm radius. The first one is correspondent to ASTM F1342 (Section 2.3.3, Fig. 2.4a). The conical probes with flat tip (Figure 4.2d) and various tip angles will be used to study the effects of tip angle on puncture resistance.

The medical needles with various tip angles α, different needle diameters (0.2 – 1.0 mm) and different hole diameters, d' (Figure 4.2e) were also used.

4.2 Tear test

As mentioned, with pointed and sharp objects, the combination of puncture and tear (or cut) may happen simultaneously. Therefore, it is necessary to determine the tearing energy or fracture energy that would be used in the puncture study of these objects.

The fracture energy or tearing energy, as mentioned in section 2.2.2, is a material property and is independent of the test piece geometry. The trouser test piece is chosen in this study because it is particularly convenient for calculating tearing energy to give more fundamental results. This test method is described in reference [29] and corresponds to the ASTM D624 – 91 [40]: Standard test method for tear strength of conventional vulcanized rubber and thermoplastic rubbers. The trouser test piece used in this study is designated as Die T in the ASTM (Figure 4.3).

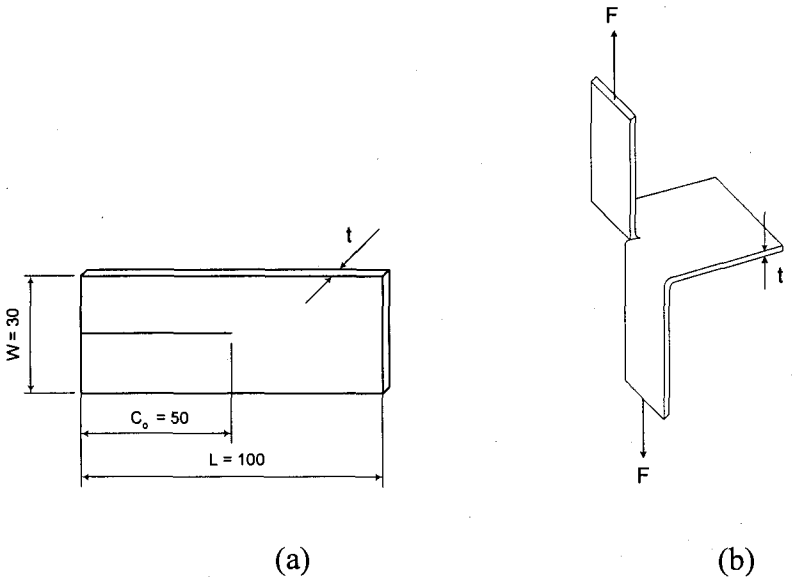

Figure 4.3: Trouser test specimen: (a) undeformed state; (b) extended state.

4.3 Tensile test (uniaxial)

The uniaxial tensile tests were done to evaluate the tensile strength of studied materials that would be used later to find out the relations to puncture resistance. This test is performed according to the ASTM standard D 412 [30], using the C type dog-bone sample. The test is carried out at room temperature, with a crosshead speed of 100 mm/min. The elongation is measured by a laser extensometer MTS LX 500 as shown in Figure 4.4.

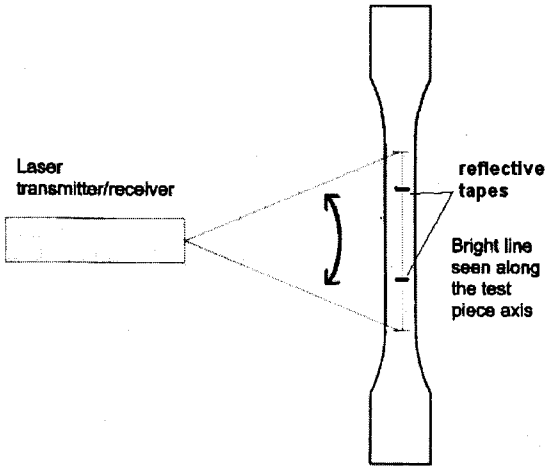

Figure 4.4: Elongation measured by laser extensometer.

4.4 Biaxial tension test (balloon test)

The balloon tests are carried out to determine the failure strain and stress in an equi-biaxial state (Figure 4.5). The pressure is measured and controlled by pressure gauge, the maximum diameter of balloon before bursting was recorded by laser extensometer MTS LX 500. The failure strain and stress are calculated by [31, 32]:

Engineering strain and stress:

$$e = \lambda - 1$$

$$\sigma_e = RP/2t \qquad (4.1)$$

with λ is the stretch ratio, $\lambda^2 = S_{ball}/S_0$

where R is the maximum radius of the balloon at burst, P is the maximum pressure, t is the initial thickness, S_{ball} is the maximum surface area of the balloon at burst, and S_0 is the initial surface of the sample.

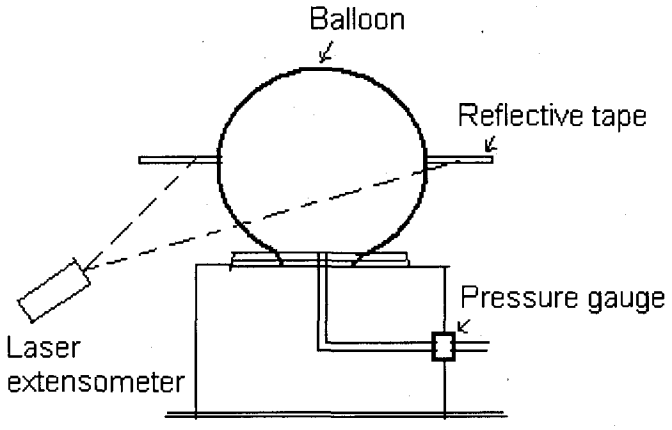

Figure 4.5: Balloon type equi-biaxial extension equipment.

True strain and stress:

$\varepsilon = \ln(e + 1) = \ln\lambda$

$\sigma = \lambda^2\sigma_e = \lambda^2 RP/2t$ (4.2)

CHAPTER 5: ARTICLE I

PUNCTURE CHARACTERIZATION OF RUBBER MEMBRANES

(CONICAL PROBES)

Date d'acception: 20 July 2004

État de l'acceptation: version finale publiée

Revue: *Theoretical and Applied Fracture Mechanics 42 (2004) p.25-33*

1. C.Thang. Nguyen, étudiant au doctorat, Université de Sherbrooke, Faculté de génie, Département de génie mécanique
2. T. Vu-Khanh*, professeur, Université de Sherbrooke, Université du Québec / École de technologie supérieure, Département de génie mécanique
3. Jaime Lara, Ph.D, Institut de recherche Robert-Sauvé en santé et en sécurité du travail, 505 de Maisonneuve Ouest, Montreal, QC, Canada, H3A 3C2

Référence : Nguyen C T, Vu-Khanh T, Lara J (2004) *Puncture characterization of rubber membranes.* Theoretical and Applied Fracture Mechanics 42: p.25-33

Titre français: Caractérisation de la perforation des membranes de caoutchouc

* toan.vu-khanh@etsmtl.ca

Abstract

Puncture resistance is among the major mechanical properties of rubber membranes, yet the intrinsic material parameters controlling the puncture of these materials are still unknown. To evaluate puncture resistance, the ASTM F1342 standard test is currently the most commonly used method. Using a conical puncture probe, this test is designed for any type of protective clothing, including coated fabrics, laminates, textiles, plastics, elastomeric films or flexible materials. This work aims to investigate the quantitative material parameters that control the puncture resistance of thin rubber membranes. Three commercial rubbers commonly used in protective gloves are investigated. The results demonstrate that the probe-tip geometry strongly affects the results in puncture characterization. The maximum puncture force depends on the contact surface between the elastomer membrane and the probe tip. The indentation force has been calculated for elastomer membranes with large deformations in the absence of friction, using the Mooney strain-energy function. The puncture strengths of elastomer membranes are much lower than their tensile and biaxial strengths. The puncture of rubber membranes is controlled by a maximum local deformation that is independent of the indentor geometry.

1. Introduction

Puncture resistance is among the major mechanical properties of protective gloves made of elastomer membranes, yet the intrinsic material parameters controlling the puncture resistance of these materials are still unknown. Various investigations have been performed on specific cases involving different materials. However, the reported investigations are either qualitative, and do not provide a fundamental understanding of the mechanisms controlling puncture, or are not applicable to the highly elastic elastomer membranes. The following section outlines the reported works on puncture involving different behaviours in various materials.

The puncture resistance of protective gloves to surgical needle was studied in [1]. In this work, 19 commercially available surgical glove liners were ranked according to a measurement of the puncture force. The resistance of finger guards, glove liners and thicker latex gloves to needle penetration were also measured in order to compare these materials in terms of puncture protection with respect to the single latex glove [2]. The effectiveness of cut-proof glove liners on cut and puncture resistance, dexterity, and sensibility are discussed in [3]. However, the thickness is not taken into account in these works, and the results are only qualitative for purposes of comparison. The puncture behaviour of rigid plaques such as polycarbonates and acrylics is reported in [4, 5]. In these works, the energy required to perforate the plaque and the peak load recorded in the puncture tests were used to characterize puncture performance. The maximum load was found to vary linearly with both the plunger diameter and the sample thickness, but no quantitative analysis of the results was performed. More fundamental investigations on puncture have been carried out on rubber blocks by fracture mechanics [6]. With a cylindrical indentor, it was has been shown that a starter crack initiates as a ring on the rubber-block surface before puncture occurs. Using fracture mechanics, a method has been developed to calculate the fracture energy in puncture. The puncture energy values obtained were found to agree with the catastrophic tearing energy obtained from trouser tear tests. However, the rubber-block situation involves surface indentation and is not applicable to the case of puncture of elastomer membranes. The quantitative characterization of puncture resistance has also been developed for geotextiles and geomembranes. In these materials, a correlation was found between the puncture force

and the tensile strength for probes greater than 20 mm in diameter [7-9]. Considering a loading state of pure axisymmetric tension, the puncture resistance of geotextile membranes was calculated in term of tensile wide-width strength. To simulate the actual application in service, the puncture of pre-strained geotextiles was also analyzed in [10] and the relationship between puncture resistance and tensile wide-width strength was confirmed. However, the results are only applicable in the case of linearly elastic deformation. Thin rubber membranes are for their part hyperelastic, and highly nonlinear.

Presently, to evaluate the puncture resistance of elastomer membranes, the standard ASTM F1342 and ISO 13996 tests are the most commonly used methods. These tests were developed to evaluate the puncture resistance of thin flexible-materials. The ASTM F 1342 [11] is designed for any type of protective clothing, including coated fabrics, laminates, textiles, plastics, elastomeric films or flexible materials. This test method determines the puncture resistance of a material specimen by measuring the maximum force required for a conical puncture probe to penetrate through a specimen clamped between two plates with chamfered holes not less than 10 mm in diameter. The aim of this work is to investigate the material parameters that control the puncture resistance of thin rubber membranes in the ASTM standard F 1342. Both the test and the mechanisms of puncture are analyzed in order to find the intrinsic parameters controlling puncture. The effects of probe geometry, and the correlations with other mechanical performances are also investigated.

2. Experimental

2.1. Materials

Three types of commercial rubbers commonly used for protective gloves, neoprene, nitrile, and natural rubber, were investigated. Neoprene sheets with three different thicknesses, 0.40, 0.78 and 1.57 mm, were obtained from Fairprene Industrial Products. The 0.30 mm thick nitrile samples were cut from Nitrile Gloves manufactured by Ansell Co. The 1.0 mm thick natural rubber samples were cut from NR Gloves, manufactured by Sandstrahler Co.

2.2. Puncture test

The puncture test was carried out on an Instron 1137 universal-testing machine. The puncture probes were held by a pin chuck mounted to the load cell. The elastomer sample was clamped between two steel plates under pressurized air, as shown in Figure 1. The hole of the lower plate was chamfered to avoid stress concentration.

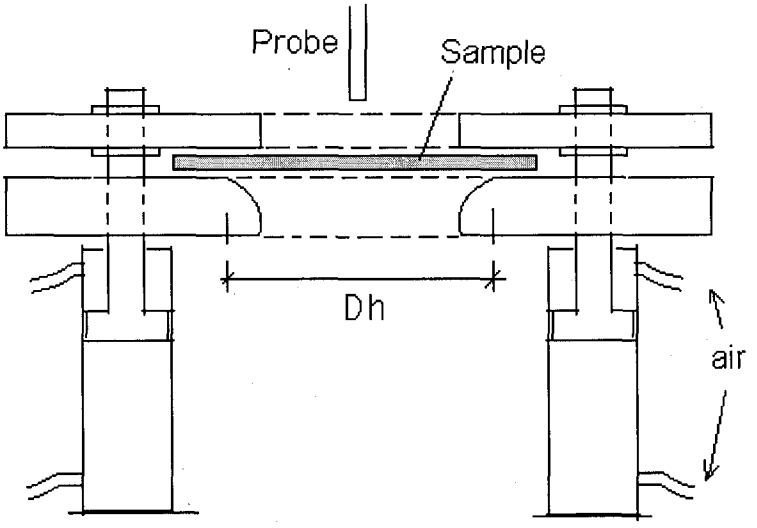

Figure 1: Sketch of sample holder

Conical probes with different cone angles and diameters are investigated in this work, as shown in Figure 2. These probes were manufactured from stainless steel.

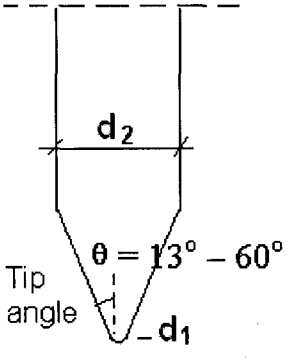

Figure 2: Conical puncture probe

2.3. Tensile test

The uniaxial tensile test was performed according to the D 412 ASTM standard [12], using the C-type dog-bone sample. The test was carried out at room temperature, with a crosshead speed of 100 mm/min. The elongation was measured by an MTS LX 500 laser extensometer.

2.4. Biaxial test

The balloon test [13, 14] was used to determine the failure stress and strain in an equibiaxial state (Figure 3). The pressure was measured using a pressure gauge while the maximum diameter of the balloon before burst was recorded through an MTS LX 500 laser extensometer.

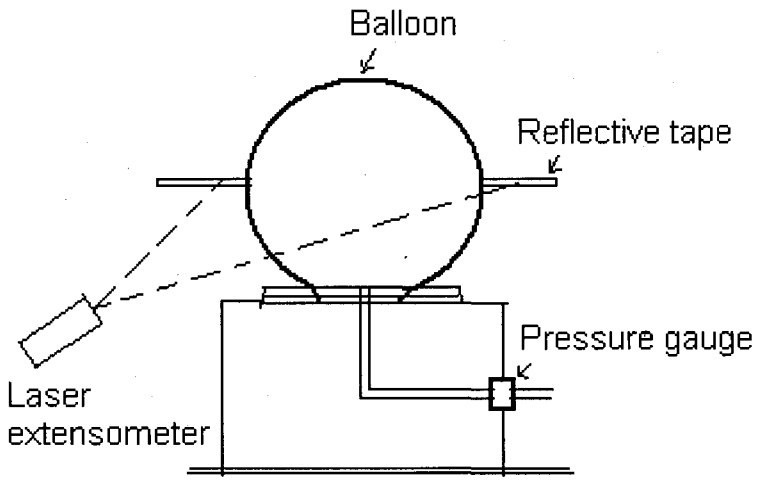

Figure 3: Balloon type equibiaxial extension equipment

3. Results and discussions

Figure 4 shows the typical curves of force versus vertical displacement recorded during the puncture tests. These curves are not linear, and show a maximum force (F) and a maximum vertical displacement (H) at puncture. Figure 5 shows the effect of the probe-tip angle on the puncture resistance of the neoprene sheet with a thickness of t = 0.78 mm. The conical probes had the same rod diameter d_2 = 1.05 mm, and the same tip diameter, d_1 = 0.05 mm, but different probe-tip angles (see Figure 2), which were $\theta = 13^\circ$, 30°, 45°, and 60°.

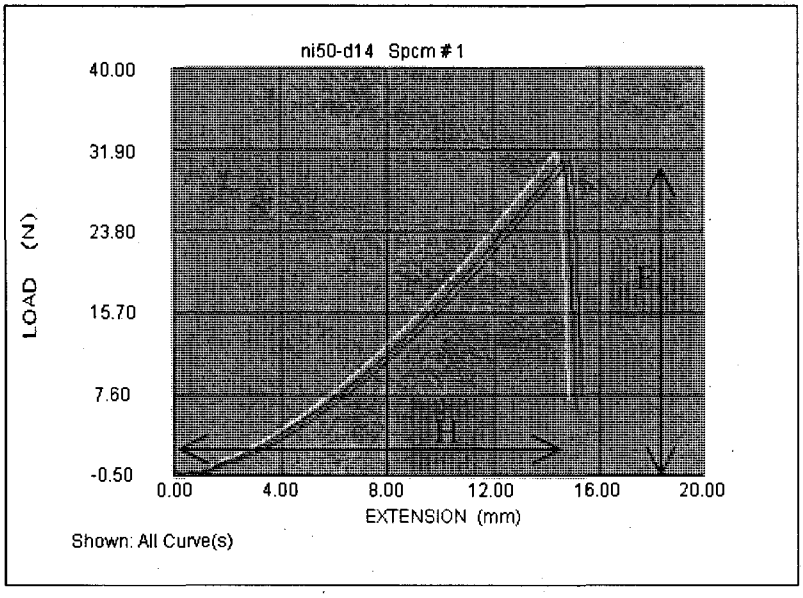

Figure 4: Typical diagram of force vs. vertical displacement for 0.3 mm thick Nitrile samples.

The results show that the puncture force strongly increases with the probe-tip angle. The same figure also shows the results obtained with two cylindrical probes with diameters of 0.05 mm and 1.05 mm. These cylindrical probes respectively correspond to the cases of $\theta = 0^\circ$ and $\theta = 90^\circ$. The measurements suggest that within the experimental error margin, the maximum puncture force obtained with the cylindrical probes fall on the same curve as that obtained with the conical probes.

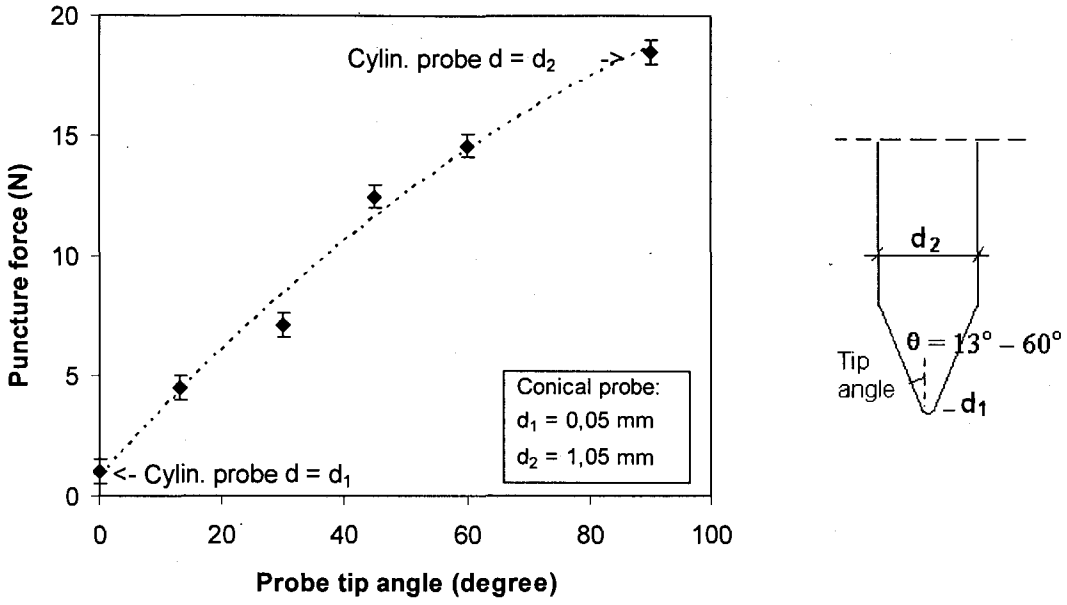

Figure 5: Variation of maximum puncture force in 0.78 mm thick Neoprene as a function of probe-tip angle.

Table 1: Failure true stress of tensile and puncture tests (in parenthesis: SD - standard deviation)

Material	Nitrile	Neoprene	NR
Failure true stress (MPa)			
Tensile	210 *(22)*	71 *(7)*	325 *(31)*
Puncture	128 *(18)*	45 *(7)*	104 *(11)*

Table 1 shows the comparison between the measured tensile stress and the maximum stress in the puncture of elastomer membrane, calculated from maximum puncture force. The maximum stress in puncture appears to be much smaller than the maximum tensile stress. Observations of the deformations of the sample before puncture revealed that at the top surface of the probe tip, the deformation is at a maximum, and is in an equibiaxial state (Figure 6). Since puncture involves a biaxial state of stress, it is relevant to verify whether these discrepancies can be due to the effect of biaxial stress. To determine the maximum

equibiaxial strength, the elastomer membranes were air-inflated until they burst. The pressure was measured and controlled using a pressure gauge while the maximum diameter of the balloon before burst was recorded through an MTS LX 500 laser extensometer. The true failure strain and stress were calculated by [13, 14]:

$$\lambda^2 = S_{ball}/S_0 \quad \text{and} \quad \sigma = \lambda^2 RP/2t \tag{1}$$

where R is the maximum radius of the balloon at burst, P is the maximum pressure, t is the initial thickness, S_{ball} is the maximum surface area of the balloon at burst, and S_0 is the initial surface of the sample.

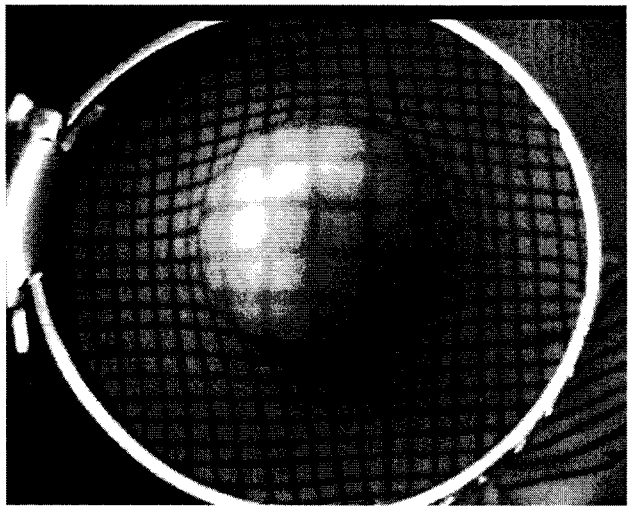

Figure 6: Biaxial deformation at probe-tip surface.

Table 2 shows the comparison between the equibiaxial and the calculated maximum puncture stresses of different elastomer membranes. The results show that the puncture strength is also smaller than the biaxial strength.

The comparison between the maximum deformations measured in puncture, tensile, and equibiaxial tests is shown in Table 3. The results once again confirm that puncture is controlled by a maximum local deformation of the membrane at the probe tip. This deformation is much smaller than the maximum tensile and equibiaxial deformations.

Table 2: Failure true stress of equibiaxial and puncture tests (in parenthesis: SD)

Material	Nitrile	Neoprene	NR
Failure true stress (MPa)			
Biaxial	270 *(29)*	73 *(9)*	317 *(35)*
Puncture	128 *(18)*	45 *(7)*	104 *(11)*

Table 3: Failure engineering strain and true strain of tensile biaxial balloon tests compared to puncture tests (in parenthesis: standard deviation)

Material	Nitrile	Neoprene	NR
Failure engineering strain (%)			
Tensile	410 *(22)*	376 *(18)*	971 *(51)*
Biaxial	239 *(17)*	186 *(16)*	493 *(42)*
Puncture	132 *(11)*	146 *(7)*	318 *(23)*
Failure true strain (%)			
Tensile	163 *(10)*	156 *(8)*	237 *(14)*
Biaxial	122 *(9)*	105 *(9)*	178 *(15)*
Puncture	84 *(8)*	90 *(5)*	143 *(12)*

Observations revealed that the elastomer membrane adheres to the probe over a specific distance from the probe tip before puncture (Figure 7). The measured puncture force thus results from the contact force at the probe. From the deformations of the elastomer

membrane shown in Figure 7, it could be assumed that the contact force would include both normal and tangential forces due to friction. In order to verify the contribution of the tangential force due to friction, puncture tests with lubricated probe tips were performed, and the results revealed that friction played only a minor role in puncture. The maximum puncture force in the presence of a lubricant was only slightly reduced (less than 6%). The maximum force measured in the puncture tests was therefore due to the normal pressure of the elastomer membrane on the probe tip.

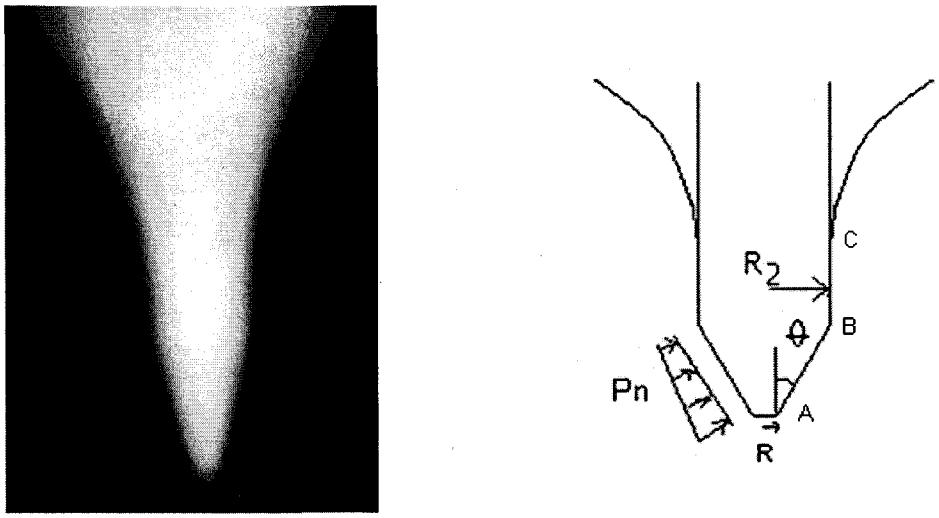

Figure 7: Deformation of elastomer membranes using puncture.

Large deformations in the indentations of circular elastic membranes by a spherical indentor in the absence of friction have been analyzed in [15]. Using a similar analysis, an attempt is made in this work to calculate the theoretical puncture force for the conical probe-tip geometry. A point P' on the deformed membrane can be described by two coordinates: ρ, the distance from the point to the axis of symmetry, and ξ, the meridian arc length between the centre of the membrane and the point shown in Figure 8. The solution of the deformed membrane is in the form:

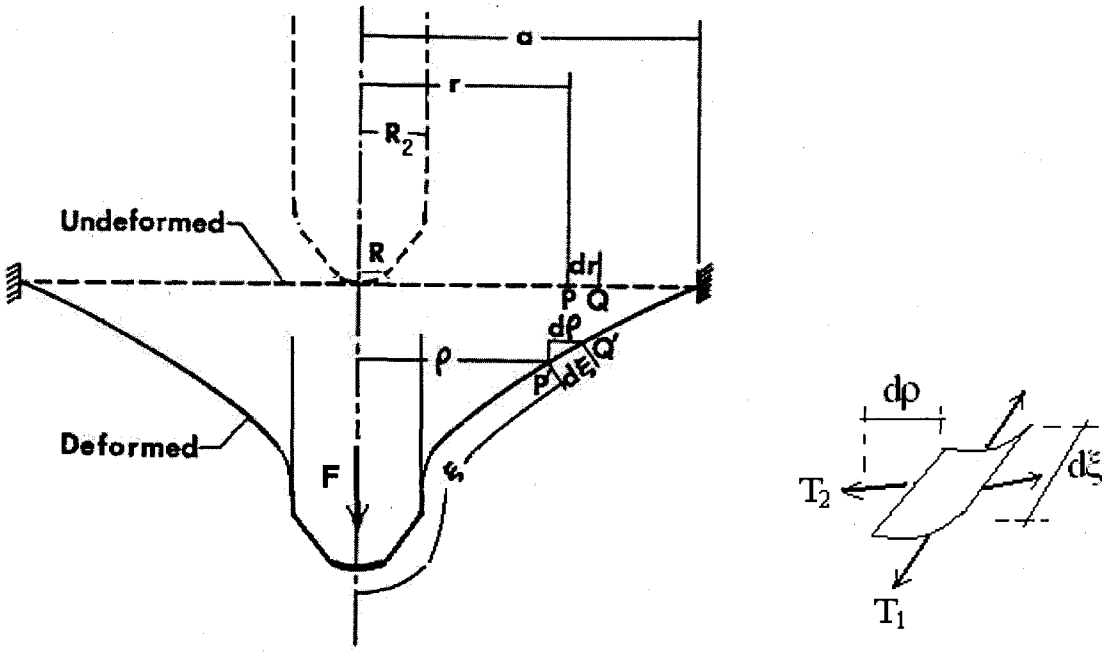

Figure 8: Coordinates in indentation of circular elastic membrane with conical probe.

$$\xi = \xi(r) \text{ and } \rho = \rho(r) \qquad (2)$$

where r is the coordinate of the point P on the undeformed membrane (corresponding to the point P' on the deformed membrane). The meridian and circumferential stretch-ratios of the deformed membrane are thus, respectively, $\lambda_1 = d\xi/dr$ and $\lambda_2 = \rho/r$. There are two distinct regions on the deformed membrane, the region which is in contact with the puncture probe, called the *contact* region, and the other, called the *non-contact* region.

In the ***non-contact region***, since it has no external load, the equations of equilibrium in the meridian and normal directions are:

$$\frac{dT_1}{d\rho} + \frac{1}{\rho}(T_1 - T_2) = 0, \qquad K_1 T_1 + K_2 T_2 = 0 \qquad (3)$$

where T_1 and T_2 are respectively the stress resultants per unit edge length in the meridian and circumferential directions, and K_1 and K_2 are the principal curvatures of the arcs in the

corresponding directions. Since elastomer membranes are elastic, isotropic and incompressible, their mechanical property can be described by the well-known Mooney strain-energy function [16]:

$$W(I, II) = C_1(I-3) + C_2(II-3) = C_1(I-3 + \alpha(II-3)) \qquad (4)$$

where the strain invariants are $I = \lambda_1^2 + \lambda_2^2 + \lambda_1^{-2}\lambda_2^{-2}$, $II = \lambda_1^{-2} + \lambda_2^{-2} + \lambda_1^2\lambda_2^2$, $III = \lambda_1\lambda_2\lambda_3 = 1$, and C_1, C_2 are material constants, and $\alpha = C_2/C_1$. From this function, the stress as a function of stretch-ratio, can be derived, respectively:

$$\sigma_1 = \frac{\partial W}{\partial \lambda_1} = \frac{\partial W}{\partial I}\frac{\partial I}{\partial \lambda_1} + \frac{\partial W}{\partial II}\frac{\partial II}{\partial \lambda_1} = \frac{\partial W}{\partial I}\left(2\lambda_1 - 2\lambda_1^{-3}\lambda_2^{-2}\right) + \frac{\partial W}{\partial II}\left(-2\lambda_1^{-3} + 2\lambda_1\lambda_2^2\right)$$

$$= 2\lambda_2\left(\frac{\lambda_1}{\lambda_2} - \lambda_1^{-3}\lambda_2^{-3}\right)\left(\frac{\partial W}{\partial I} + \lambda_2^2\frac{\partial W}{\partial II}\right) = 2\lambda_2\left(\frac{\lambda_1}{\lambda_2} - \lambda_1^{-3}\lambda_2^{-3}\right)\left(C_1 + \lambda_2^2 C_2\right) \qquad (5)$$

The stress resultants per unit edge length in the meridian and circumferential directions, are respectively:

$$T_1 = \sigma_1^{true} h_{deformed} = \sigma_1\lambda_1 h\lambda_3 = \sigma_1\lambda_1\frac{h}{\lambda_1\lambda_2} = \frac{\sigma_1 h}{\lambda_2}; \qquad (III = \lambda_1\lambda_2\lambda_3 = 1 \rightarrow \lambda_3 = 1/\lambda_1\lambda_2)$$

$$= \frac{\sigma_1 h}{\lambda_2} = 2hC_1\left(\frac{\lambda_1}{\lambda_2} - \lambda_1^{-3}\lambda_2^{-3}\right)\left(1 + \lambda_2^2\alpha\right)$$

and

$$T_2 = \frac{\sigma_2 h}{\lambda_1} = 2hC_1\left(\frac{\lambda_2}{\lambda_1} - \lambda_1^{-3}\lambda_2^{-3}\right)\left(1 + \lambda_1^2\alpha\right) \qquad (6)$$

where h is the undeformed thickness of the membrane.

By introducing three variables $x = d\rho/dr$, $\lambda_1 = d\xi/dr$ and $\lambda_2 = \rho/r$, and substituting these equations into Equation (3), the governing differential equations for the variables, x, λ_1, λ_2 in the non-contact region can be obtained.

In the ***contact region***, the membrane conforms to the surface profile of the probe, which is a known surface. Hence, ξ and ρ are related by the equation of the probe surface. The puncture force includes: $F = F_1 + F_2$, where F_1 is due to the pressure under the probe tip, and F_2 is due to the pressure between the conical surface of the probe tip and the membrane (the region between point 'A' and point 'B' in Figure 7). F_1 and F_2 are calcculated as follows:

The contact region under the probe tip is in an equibiaxial stress state: $\lambda_1 = \lambda_2 = \lambda_0$, and r at the point A (Figure 7) is determined by: $r_1 = R/\lambda_0$ ($\lambda_2 = \rho/r = R/r$). The pressure distribution between the probe tip and the membrane in this region is:

$$p_n = K_1T_1 + K_2T_2 \tag{7}$$

where $K_1 = K_2 = 1/R$;

$$\text{and } T_1 = T_2 = C_1 2h\left(1 - \frac{1}{\lambda_0^6}\right)(1 + \alpha\lambda_0^2) \tag{8}$$

The force F_1 can thus be expressed as a function of the stretch ratio λ_0 under the probe tip by:

$$F_1 = 4R^2p_n = \quad 16RC_1h\left(1 - \frac{1}{\lambda_0^6}\right)(1 + \alpha\lambda_0^2) \tag{9}$$

For F_2, the vertical force component due to the pressure in the zone AB (Figure 7) is:

$$F_2 = A\, p_n{}^{ave.} \sin\theta = \pi\left(R_2^2 - R^2\right) p_n{}^{ave.} \tag{10}$$

where A is the area of the conical surface (zone AB in Figure 7): $A = \frac{\pi}{\sin\theta}\left(R_2^2 - R^2\right)$

The average pressure $p_n{}^{ave}$ in the zone AB is:

$$p_n{}^{ave.} = \overline{K}_1\overline{T}_1 + \overline{K}_2\overline{T}_2 \tag{11}$$

where $\overline{K}_1 = 0$, $\overline{K}_2 = 2\cos\theta/(R_2 + R)$ -> $p_n^{ave.} = 2\cos\theta/(R_2 + R)\overline{T}_2$

and $\overline{T}_2$ is the average values of T_2 in the zone AB:

$$\overline{T}_2 = C_1 2h\left[\frac{\overline{\lambda}_2}{\overline{\lambda}_1} - \frac{1}{\overline{\lambda}_1^3 \overline{\lambda}_2^3}\right]\left(1 + \lambda_1^2\alpha\right) \tag{12}$$

where $\overline{\lambda}_1, \overline{\lambda}_2$ are the average values of λ_1, λ_2 in the zone AB (Figure 7).

In the contact region BC (between point B and point C in Figure 7), there results:

$$\begin{aligned} &\rho = R_2 \\ &x = d\rho/dr = 0 \\ &\lambda_2 = \rho/r = R_2/r \\ &K_1 = 0 \text{ and } K_2 = 1/R_2 \end{aligned} \tag{13}$$

The total load at each cross-section remains unchanged, and is equal to the total load F exerted by the probe. Since T_2 is perpendicular to F, by substituting $\lambda_2 = \rho/r = R_2/r$, this leads to:

$$F = 2\pi\rho\, T_1 = 2\pi R_2 2h\, C_1\left[\lambda_1\left(\frac{r}{R_2}\right) - \lambda_1^{-3}\left(\frac{r}{R_2}\right)^3\right]\left(1 + \alpha\left(\frac{R_2}{r}\right)^2\right) \tag{14}$$

where $F = F_1 + F_2$.

Figure 9 shows a schematic representation of the variation of λ_1 and λ_2 with r. At r = a, the clamping sample holder (Figure 8), $\lambda_{2\,(r\,=\,a)} = 1$. The radius r_3 in the underformed membrane, corresponding to the point C after deformation, can be determined by iteration with the continuity conditions:

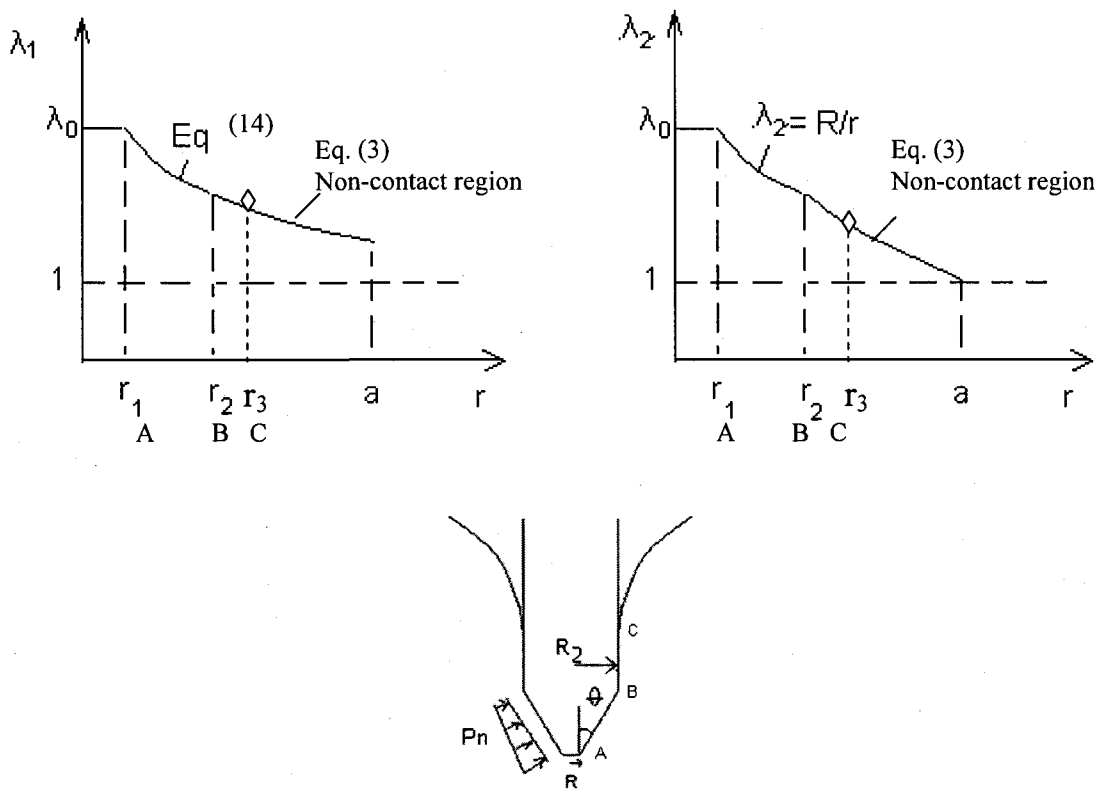

Figure 9: Schematic variation of λ_1 and λ_2 with r.

Eqs. (14) and Eqs. (3) give: $\lambda_1(r_3)_c = \lambda_1(r_3)_{nc}$ (15)

Eqs. (13) and Eqs. (3) render: $\lambda_2(r_3)_c = \lambda_2(r_3)_{nc}$ (16)

where the *c* and *nc* subscripts denote the quantities being obtained from the *contact* and *non-contact regions*, respectively. For an approximate value of λ_{10} (λ_1 *at* $r = a$), we can find r_3^a and r_3^b that satisfy Equations 15 and 16 respectively. If $|r_3^a - r_3^b|/r_3^a > 0.001$, take $r_3 = (r_3^a + r_3^b)/2$, recalculate Equations 3 and get the new λ_{10}, the iteration was performed until $|r_3^a - r_3^b|/r_3^a < 0.001$.

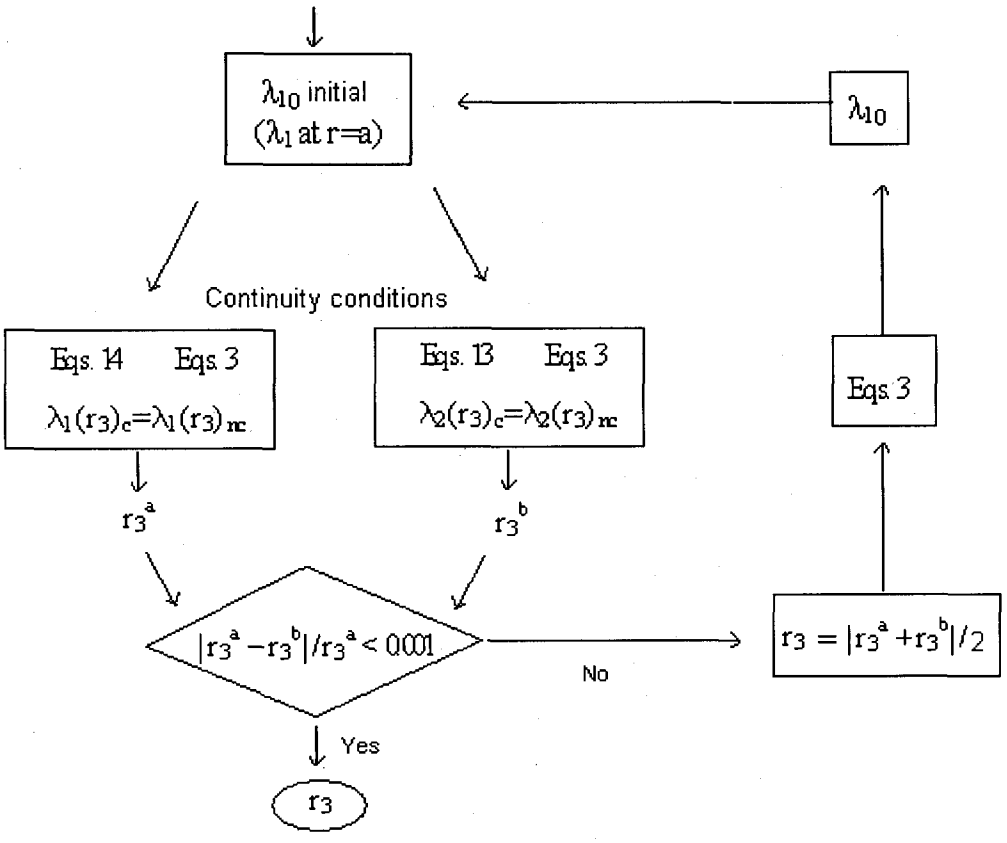

When r_3 is determined, the radius r_2 in the undeformed membrane, corresponding to the point B after deformation, and $\bar{\lambda}_1, \bar{\lambda}_2$ in Equation 9 can be calculated. The correct value of F_2 is obtained by Equation 10. Then the puncture force can be computed by $F = F_1 + F_2$ where F_1 and F_2 are calculated by Equation 9 and 10 respectively or F can be obtained by Equation 14.

For the conical probes with $\theta = 13^\circ$, $d_2 = 2.0$ mm, the calculated puncture force and experimental results of these probes for Nitrile and NR are shown in Figures 10 and 11 respectively.

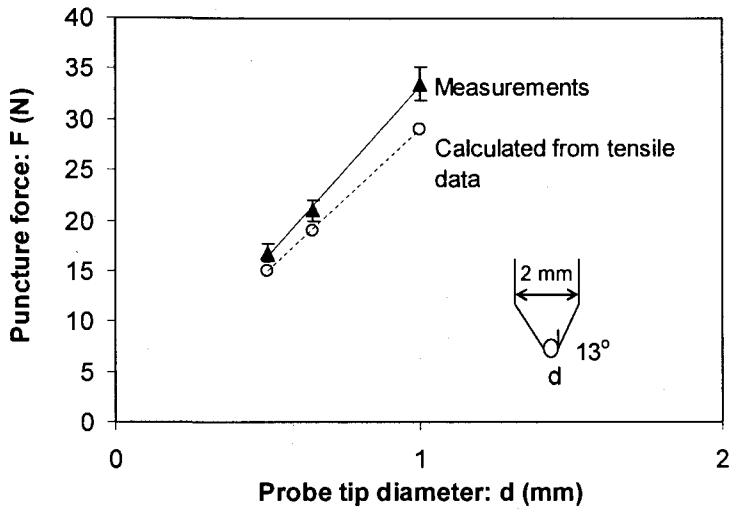

Figure 10: Calculated and measured puncture force as a function of probe-tip diameter in 0.3 mm thick Nitrile sample (C_1 = 902 kPa, α = 0.28).

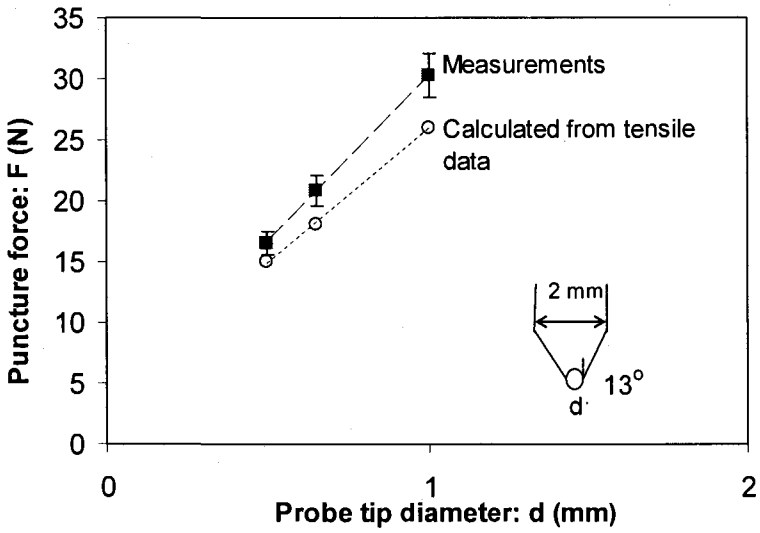

Figure 11: Calculated and measured puncture force as a function of probe-tip diameter in 1.0 mm thick natural rubber sample (C_1 = 70 kPa, α = 2.96).

The calculated puncture force of the conical probes is smaller than that obtained from experimental results (7% - 15%). This is probably because the Mooney function is only accurate for strains less than about 100% [16]. Figure 12 shows the comparison between the

Mooney function and the experimental data of tensile tests on neoprene samples. It can be seen that above about 100%, the discrepancy between Mooney's function and experimental data strongly increases with stretch ratio. Since the failure strain in the puncture is about 135% to 320% for the rubbers studied, the error of Mooney's function becomes significant.

Other material models for rubber are more precise (up to 250% of strain), but they have many parameters (> 2), therefore the computation process will be more complicated. In the future works, Mooney's model will be replaced by other precise material model.

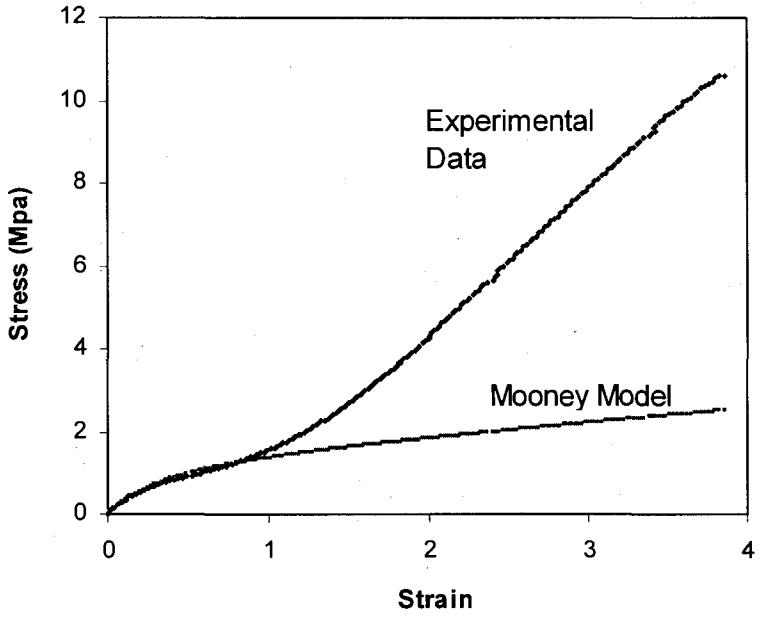

Figure 12: Stress-strain behavior of neoprene using tensile test.

5.4 Conclusion

It has been demonstrated in this work that the geometry and dimensions of the probe used in the F1342 ASTM standard strongly affects the results of the puncture characterization of elastomer membranes. The maximum puncture force depends on the contact surface between the elastomer membrane and the probe tip. The indentation force has been calculated for large deformations in the absence of friction using the Mooney strain-energy function. The calculation agrees with experimental measurements within the range of accuracy of the Mooney strain-energy function. The puncture strength is much smaller than both the tensile and the biaxial stresses. The maximum stress in puncture corresponds to the maximum strains measured from the top surface of the probe. The puncture of the elastomer membrane is controlled by a local deformation that is an intrinsic material parameter, and is independent of the indentor geometry.

Acknowledgements

The authors would like to thank the Institut de recherche Robert-Sauvé en santé et en sécurité du travail (IRSST) du Québec for their financial support provided for this work.

References

1. L.F. Leslie, J.A. Woods, J.G. Thacker, R.F. Morgan, W. McGregor, R.F. Edlich, Needle puncture resistance of medical gloves, finger guards, and glove liners, J. Biomedi. Mater. Research 33 (1996) 41 - 46.

2. J.A. Salkin, S.A. Stuchin, F.J. Kummer, R. Reininger, The effectiveness of cut-proof glove linears: cut and puncture resistance, dexterity, and sensibility, Orthopedics: Thorofare 18 (1995) 1067 - 1071.

3. Daniel J. Hewett, Protocol for the puncture resistance of medical glove liners, National Institute for Occupational Safety and Health, USA, 1993.

4. G.R. Tryson, M.T. Takemori, A.F. Yee, Puncture testing of plastics: effects of test geometry, Amer. Soc. Mech. Eng. - AMD 35 (1979) 638 - 647.

5. L.M. Carapellucci, A.F. Yee, Some problems associated with puncture testing of plastics, Poly. Eng. Sci. 27 (1987) 773 - 785.

6. A. Stevenson, Kamarudin Ab Malek, On the puncture mechanics of rubber, Rub. Chem. Tech. 67 (1994) 743 - 760.

7. V.P. Murphy, R.M. Koerner, CBR strength (Puncture) of geosynthetics, Geotech. Test. J. 3 (1988) 167 - 172.

8. D. Narejo, R.M. Koerner, R.F. Wilson-Fahmy, Puncture protection of geomembrances, Part II: experimental, Geosynthetics Inter. 3 (1996) 629 - 653.

9. R.F. Wilson-Fahmy, D. Narejo, R.M. Koerner, Puncture protection of geomembrances, Part I: theory, Geosynthetics Inter. 3 (1996) 605 - 628.

10. Tushar K. Ghosh, Puncture resistance of pre-strained geotextiles and its relation to uniaxial tensile strain at failure, Geotextiles and Geomembrances 16 (1998) 293 - 302.

11. ASTM F1342 "Standard Test method for Protective Clothing Material Resistance to Puncture", Annual Book of ASTM Standards 11.03, USA, 1999.

12. ASTM D412 "Standard Test Methods for Vulcanized Rubber and Thermoplastic Elastomers - Tension", Annual Book of ASTM Standards 9.01, USA, 1998.
13. Y. Yoshihiro, K. Sueo, T. Yuji, S. Wataru, Biaxial Extension Strength of Carbon Black Reinforced Rubber, Nihon Gomu Kyokaishi 67 (1994) 576 - 587.
14. Sueo Kawataba, Fracture and mechanical behavior of rubber-like polymers under finite deformation in biaxial stress field, J. Macromol. Sci. - Phys. B8(3) (1973) 605 - 630.
15. W.H. Yang, K.H. Hsu, Indentation of a circular membrane, J. App. Mech. 38 (1971) 227 -230.
16. M. Mooney, A theory of large elastic deformation, J. App. Phys. 11 (1940) 582 - 592.

CHAPTER 6: ARTICLE II

MECHANICS AND MECHANISMS OF PUNCTURE OF ELASTOMER MEMBRANES

(CYLINDRICAL PROBES)

Date d'acception: 3 June 2004
État de l'acceptation: version finale publiée
Revue: *Journal of Materials Science 39 (2004) p.7361-7364*

1. C.Thang. Nguyen, étudiant au doctorat, Université de Sherbrooke, Faculté de génie, Département de génie mécanique
2. T. Vu-Khanh*, professeur, Université de Sherbrooke, Université du Québec / École de technologie supérieure, Département de génie mécanique

Référence : Nguyen C T, Vu-Khanh T (2004) *Mechanics and mechanisms of puncture of elastomer membranes*. Journal of Materials Science 39(24): p.7361-7364

Titre français: Mécaniques et mécanismes de la perforation de membranes élastomères

* toan.vu-khanh@etsmtl.ca

Introduction

Regardless of their importance, the intrinsic material parameters controlling the puncture resistance of elastomer membranes are still unknown. Various investigations have been performed on specific cases involving different materials. However, the reported investigations are either qualitative, and do not provide a fundamental understanding of the mechanisms controlling puncture, or are not applicable to the highly elastic elastomer membranes. The puncture resistance of protective gloves to surgical needles was studied in [1, 2]. In these works, 19 commercially available surgical glove liners were qualitatively ranked according to a measurement of the puncture force, in order to compare these materials in terms of puncture protection with respect to the single latex glove. The puncture behaviour of rigid plaques such as polycarbonates and acrylics is reported in [3, 4]. In these works, the energy required to perforate the plaque and the peak load recorded in the puncture tests were used to characterize puncture performance. However, the thickness was not taken into account, and no quantitative analysis of the results was performed. More fundamental investigations on puncture have been carried out on rubber blocks by fracture mechanics [5]. With a cylindrical indentor, it was shown that a starter crack initiates as a ring on the rubber-block surface before puncture occurs. Using fracture mechanics, a method has been developed to calculate the fracture energy in puncture. However, this situation is not applicable to thin elastomer membranes. In fact, a quantitative characterization of puncture resistance has been developed for geotextiles and geomembranes. Considering a loading state of pure axisymmetric tension, a correlation was found between the puncture force and the tensile strength for probes greater than 20 mm in diameter [6 - 9]. However, the results are only applicable in the case of linearly elastic deformation. Thin rubber membranes are for their part hyperelastic, and highly nonlinear.

To evaluate puncture resistance, the ASTM F1342 standard test is currently the most commonly used method. Using a conical puncture probe, the test is designed for any type of protective clothing, including coated fabrics, laminates, textiles, plastics, elastomeric films or flexible materials. This test method determines the puncture resistance of a material by measuring the maximum force required for a conical puncture probe to penetrate through a

specimen clamped between two plates with chamfered holes not less than 10 mm in diameter. In a previous investigation, it was found that the probe tip geometry strongly affects the results in puncture characterization. The maximum puncture force depends on the contact surface between the elastomer membrane and the probe tip. The indentation force was calculated for elastomer membranes with large deformations in the absence of friction, using the Mooney strain-energy function. The puncture strengths of elastomer membranes were found to be much lower than their tensile and biaxial strengths. It was also found that the puncture of rubber membranes is controlled by a local equibiaxial deformation on the probe tip, which is independent of the indentor geometry. To find the intrinsic parameters controlling puncture performance, accurate measurements of the equibiaxial deformation on the surface of the probe tip, at the onset of puncture, must be performed. Since the conical probe used in the ASTM F1342 standard is also very costly to produce, it is interesting to find an alternative, simpler, and quantitative measurement not requiring any major modifications of this standard. Since the previous result suggested that there would be a unique relationship between the puncture force and the probe-tip angle, the focus of this work is concentrated on the puncture mechanisms of elastomer membranes by cylindrical probes with both flat and rounded tips.

Three types of commercial rubbers commonly used for protective gloves, neoprene, nitrile, and natural rubber, were investigated. Neoprene sheets with three different thicknesses, 0.40, 0.75 and 1.57 mm, were obtained from Fairprene Industrial Products. The 0.30 mm thick nitrile samples were cut from Nitrile Gloves manufactured by Ansell Co, and the 1.0 mm thick natural rubber samples were cut from NR Gloves, manufactured by Sandstrahler Co. The puncture tests were carried out on an Instron 1137 universal-testing machine. A pin chuck mounted on the load cell held the puncture probes. The elastomer sample was clamped between two steel plates under pressurized air, as shown in Figure 1a. The hole of the lower plate was chamfered to avoid stress concentration. The cylindrical probes with flat and rounded tips are shown in Figures 1b & c.

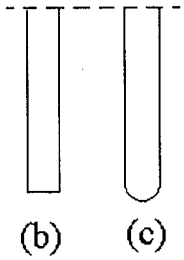

Figure 1: Sketch of sample holder (a); cylindrical probes with flat tip (b) and cylindrical probes with rounded tip (c).

Results and discussions

Figure 2 shows the deformations of the elastomer membrane for the cylindrical probes, with rounded and flat tips. It can be seen that in all geometries, the elastomer membrane always adheres to the probe tip over a certain distance with an equibiaxial

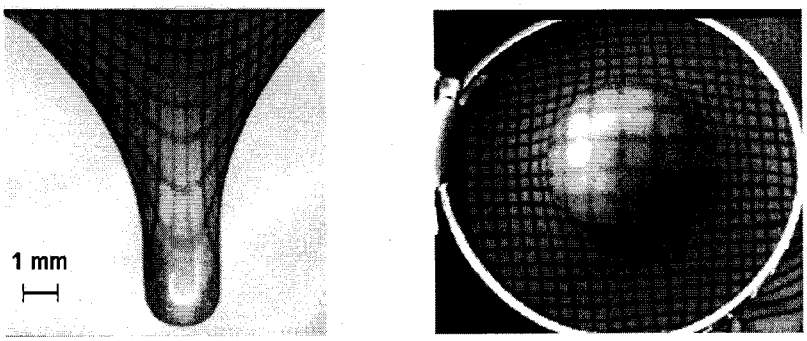

a) cylindrical probe: rounded tip

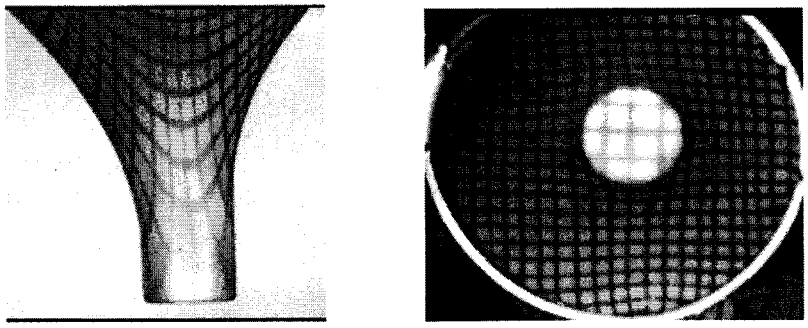

b) cylindrical probe: flat tip

Figure 2: Deformations of the elastomer membrane for the cylindrical probes: rounded tip (a) and flat tip (b).

deformation on the probe-tip surfaces. The effect of probe radius on the maximum puncture force is shown in Figure 3. The results suggest a linear relationship between the maximum puncture forces and the probe radius for the three elastomers tested. Figure 4 shows the normalized maximum force *F/t* as a function of the probe diameter for the neoprene sheets of three different thicknesses. It can be seen that the maximum puncture force is proportional to the sheet thickness and the probe diameter.

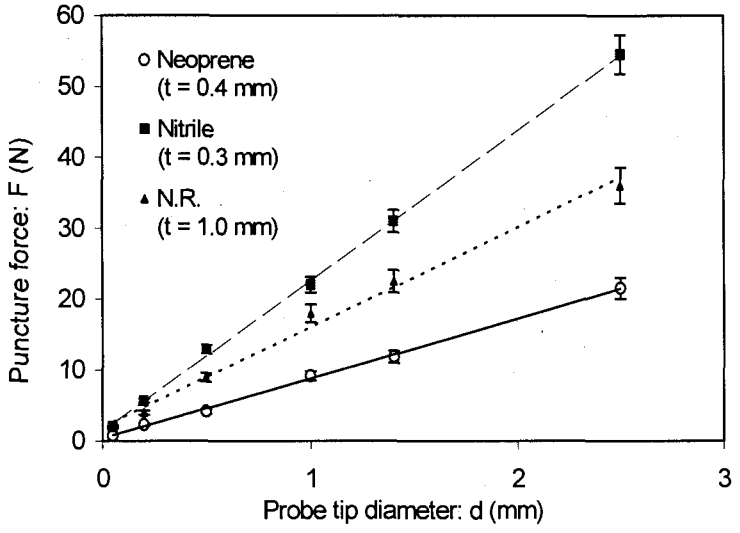

Figure 3: Plots of puncture force versus probe tip diameter for various rubbers.

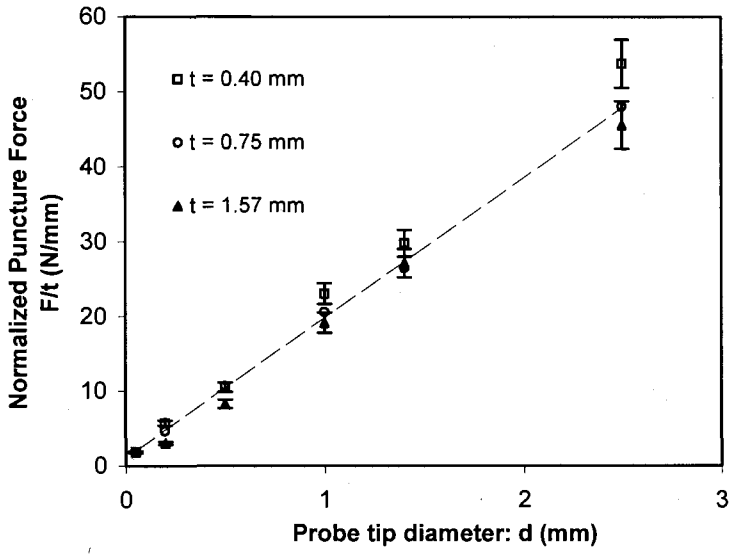

Figure 4: Normalized puncture force as a function of probe tip diameter for Neoprene sheets at different thicknesses.

The results seem to suggest that the puncture behavior of elastomers is controlled by the same material parameter as that of geotextile membranes. The puncture resistance of these materials has been shown to be controlled by their tensile strength, and is given by [5, 6]:

$$T_f = F_p / 2\pi r \qquad (1)$$

where T_f is the tensile strength per unit width of fabric (kN/m), r is the radius of the probe (m) and F_p is the puncture force (kN). Table 1 shows the comparison between the measured tensile and puncture strengths of different elastomers, suggesting that unlike in the case of geotextile membranes, the puncture strength is much smaller than the tensile strength, thus refuting the criterion controlling the puncture resistance of geotextile membranes.

Table 1: Failure engineering stress and true stress of tensile and puncture tests (in parenthesis: SD – standard deviation)

Material	Nitrile	Neoprene	NR
Failure engineering stress (MPa)			
Tensile	41 *(4)*	15 *(2)*	30 *(3)*
Puncture	55 *(7)*	18 *(2)*	25 *(3)*
Failure true stress (MPa)			
Tensile	210 *(22)*	71 *(7)*	325 *(31)*
Puncture	128 *(18)*	45 *(7)*	104 *(11)*

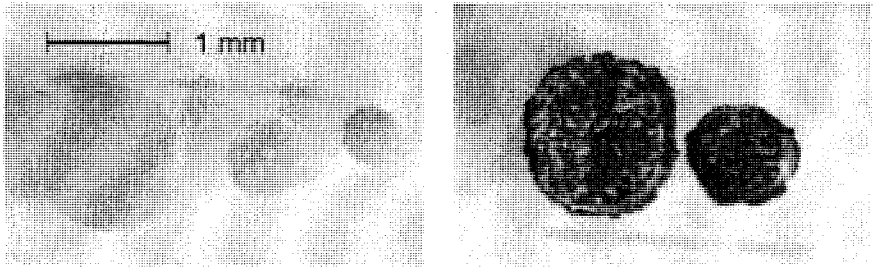

a) Nitrile b) Neoprene

Figure 5: Cut-out disks of elastomer samples after puncture (optical microscopy: 20x).

With the cylindrical probes, it is interesting to note that after puncture, a hole in the membrane having a specific diameter is always observed, and a small disk is cut out from the rubber membrane as shown in Figure 5. The diameter of the cut-out disks, d_f, depends on the probe diameter d, and is always smaller than that of the probe ($d_f < d$). From the deformation observed in Figure 2, it is reasonable to consider that puncture would take place around the circumferential edge of the cylindrical probe. The diameter of the cut-out disk at the onset of

puncture (at maximum equibiaxial deformation) would correspond to the diameter of the probe. Since the deformation is axisymmetrical, the radial strain ε_r and the tangential strain ε_t of the cut-out disk can be calculated. The extension ratios λ_r, λ_t at the radial and tangential directions are, respectively:

$$\lambda_r = d/d_f \tag{2a}$$

$$\lambda_t = \frac{\text{Circumference of cutout disk at puncture}}{\text{Circumference of cutout disk at undeformed state}} = \frac{\pi d}{\pi d_f} = \frac{d}{d_f} \tag{2b}$$

The corresponding engineering strains and true strains are therefore, respectively:

$$e_r = e_t = \lambda_t - 1 = d/d_f - 1 \tag{3a}$$

$$\varepsilon_r = \varepsilon_t = \text{Ln}\,(\lambda_t) = \text{Ln}\,(d/d_f) \tag{3b}$$

Table 2: Relations between probe tip diameter and cut-out disk diameter

Material	Nitrile			Neoprene		NR
d (mm)	1.0	1.4	2.5	1.4	2.5	2.5
d_f (mm)	0.43	0.60	1.10	0.55	1.05	0.60
d/d_f	2.32	2.33	2.30	2.54	2.40	4.16
e_r	1.32	1.33	1.30	1.54	1.40	3.16
ε_r	0.84	0.85	0.83	0.93	0.88	1.43

To verify the above assumption, the diameters of the cut-out disks were measured with an optical microscope and the results are presented in Table 2. Regardless of the probe diameter, the ratio d/d_f is constant for each material, and is very close to the equibiaxial strain measured at the onset of puncture of the elastomer membrane, on the top surface of the probe.

In order to verify whether puncture was caused by stress concentration around the circumferential edge of the cylindrical probe with a flat tip, puncture tests using a cylindrical probe with a semi-hemispherical tip were performed. Table 3 shows the comparisons of the maximum force and deformation at the probe tip between flat and hemispherical tips. It can be seen that the hemispherical geometry of the probe tip gives the same maximum puncture force and equibiaxial strain as the flat tip. It is also interesting to note that the rounded tip probe also produces a hole in the elastomer membrane with a dropout disk of the same diameter as shown in Figure 6.

Table 3: Tests results (and their SDs) for two types of puncture probe (d = 1.0 mm)

Material	Neoprene		Nitrile		NR	
Probe tip type	Flat	Rounded	Flat	Rounded	Flat	Rounded
Puncture force F_p (N)	13.5 ± 0.4	13.6 ± 0.5	21.2 ± 1.4	22.0 ± 0.9	21.0 ± 1.1	20.6 ± 1.6
Max. strain	1.46 ± 0.13	1.40 ± 0.17	1.32 ± 0.08	1.35 ± 0.10	3.18 ± 0.21	3.05 ± 0.23

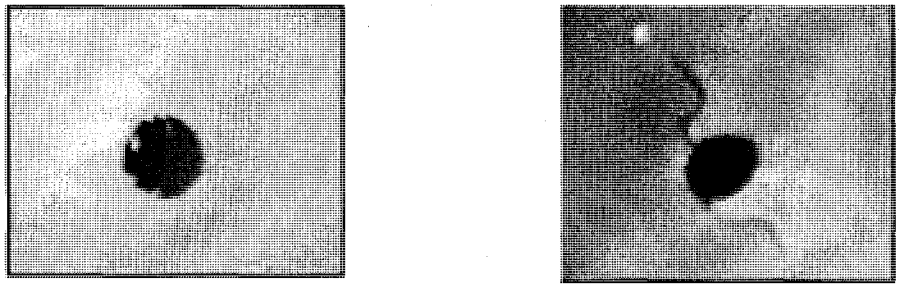

(a) (b)

Figure 6: Holes observed in the elastomer membrane after puncture: (a) flat tip and (b) rounded tip.

The result suggests that the puncture in the elastomer membrane is not due to stress concentration around the edge of the flat tip. Within the range of probe diameters investigated in this work (from 0.1 to 2.5 mm), puncture is controlled by an equibiaxial deformation that is independent of the probe diameter and geometry.

Conclusion

The above results are quite interesting for the characterization of the puncture resistance of elastomeric membranes. Indeed, a simpler cylindrical probe can be used in the place of the costly conical probe required by the ASTM Standard and will still provide a quantitative characterization of puncture. Furthermore, the rounded-tip probe gives exactly the same result as that of the flat-tip probe. Since the latter is much easier to produce, the expensive ASTM probe can be replaced by a simple flat-tip cylindrical probe. The cylindrical probe produces a hole with a dropout disk, reflecting the characteristic equibiaxial deformation controlling the puncture resistance of the elastomer membranes. This probe provides a quantitative and much simpler method for the characterization of puncture in these materials.

References

1. L. F. LESLIE, J. A. WOODS, J. G. THACKER, R. F. MORGAN, W. MCGREGOR, R. F. EDLICH, *J. Biomed. Mater. Res.* **33** (1996) 41.
2. DANIEL J. HEWETT, in "Protocol for the puncture resistance of medical glove liners" (National Institute for Occupational Safety and Health, USA, 1993) p. 31.
3. G. R. TRYSON, M. T. TAKEMORI, A. F. YEE., *Amer. Soc. Mech. Eng. - AMD* **35** (1979) 638.
4. L. M. CARAPELLUCCI, A. F. YEE, *Poly. Eng. Sci.* **27** (1987) 773.
5. A. STEVENSON, KAMARUDIN AB MALEK, *Rub. Chem. Tech.* **67** (1994) 743.
6. V. P. MURPHY, R. M. KOERNER, *Geotech. Test. J.* **3** (1988) 167.
7. D. NAREJO, R. M. KOERNER, R. F. WILSON-FAHMY, *Geosyn. Inter.* **3** (1996) 629.
8. R. F. WILSON-FAHMY, D. NAREJO, R. M. KOERNER, *Geosyn. Inter.* **3** (1996) 605.
9. TUSHAR K. GHOSH, *Geotex. and Geomem.* **16** (1998) 293.

CHAPTER 7: ARTICLE III

PUNCTURE RESISTANCE OF RUBBER MEMBRANES BY MEDICAL NEEDLES. PART I: MECHANISMS

Date d'acception: 12 Feb. 2009

État de l'acceptation: version finale publiée

Revue: *International Journal of Fracture - v.155 No.1 (2009) p.75-81*

1. C.Thang. Nguyen, étudiant au doctorat, Université de Sherbrooke, Faculté de génie, Département de génie mécanique
2. T. Vu-Khanh*, professeur, Université de Sherbrooke, Université du Québec / École de technologie supérieure, Département de génie mécanique
3. Patricia I. Dolez, Ph.D, Université de Sherbrooke, Université du Québec / École de technologie supérieure, Département de génie mécanique
4. Jaime Lara, Ph.D, Institut de recherche Robert-Sauvé en santé et en sécurité du travail, 505 de Maisonneuve Ouest, Montreal, QC, Canada, H3A 3C2

Référence : Nguyen C T, Vu-Khanh T, Dolez P I, Lara J (2009) *Puncture of elastomers membranes by medical needles. Part I: Mechanisms.* International Journal of Fracture v.155 no.1: p.75-81

Titre français: Perforation de membranes élastomères par aiguilles médicaux. Partie I: Mécanismes

* toan.vu-khanh@etsmtl.ca

Abstract

Resistance to puncture is a critical property for several applications, in particular for elastomer materials used in protective clothing. To evaluate the puncture resistance of membranes, some methods have been proposed as standard tests. However, the rounded puncture probes used in these tests are very different from real pointed objects like medical needles, and may not measure the level of material resistance that corresponds to them. In fact, puncture by medical needles is shown to proceed gradually as the needle cuts into the membrane. This behavior is highly different from puncture by rounded probes which occurs suddenly when the strain at the probe tip reaches the failure value. In addition, maximum force values are observed to be much smaller with medical needles. A method has been developed based on the change in strain energy with the puncture depth to evaluate the fracture energy associated to puncture. The results show that the phenomenon of puncture by medical needles involves contributions both from friction and fracture energy, in a similar way as for cutting. A lubricant was tentatively used to reduce the friction contribution for the computation of the material fracture energy.

Keywords

puncture, elastomer, medical needle, friction, fracture energy

1. **Introduction**

Puncture resistance is among the major mechanical properties of elastomer membranes, especially in the case of their use in protective clothing. In terms of puncture agents, medical needles are becoming an increasingly encountered mechanical hazard, not only in health care but also for law enforcement and maintenance occupations, with the associated risk of blood-borne pathogen transmission. Some investigations have been performed on specific cases using medical needles. In two studies, a total of seven commercially available surgical gloves and glove liners were tested for resistance to puncture with different types of medical needles (Leslie et al. 1996; Hewett 1993). The main goal was to rank the gloves and compare the protection efficiency of new materials with regular latex gloves. In another work, the influence of various needle characteristics on the resistance to puncture by medical needles of materials relevant to protective gloves was investigated (Dolez et al. 2008). However, these studies were only qualitative for a comparison purpose and did not provide a fundamental understanding of the mechanisms controlling puncture.

To evaluate the puncture resistance of materials, the ASTM F1342 standard test (ASTM F1342 2005) is currently the most commonly used method. This standard test method considers the use of one of three alternative puncture probes (see Figure 1); Probe A has a 2 mm diameter and a conic extremity with an angle of 26° and a rounded tip with a radius of 0.25 mm; Probe B has a 1 mm diameter and a spherical extremity with a rounded tip radius of 0.50 mm; Probe C is similar to probe A but with a rounded tip radius of 0.50 mm. The test is designed for any type of protective clothing, including coated fabrics, laminates, textiles, plastics, elastomeric films or flexible materials. This test method determines the puncture resistance of a material by measuring the maximum force required for a puncture probe that moves at a speed of 500 mm/min to penetrate through a specimen clamped between two plates with chamfered holes not more than 10 mm in diameter.

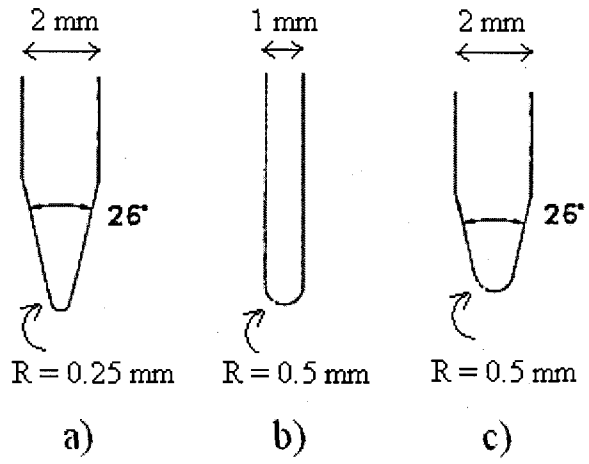

Fig. 1 Schematic representation of the ASTM F1342 probes, a) probe A, b) probe B, and c) probe C

In previous studies using rounded probes (Nguyen and Vu-Khanh 2004; Nguyen et al. 2004), it was found that the probe tip geometry strongly affects the results in puncture of elastomer membranes. The maximum puncture force depends on the contact surface between the membrane and the probe tip. Using the Mooney strain-energy function, the indentation force was calculated for elastomer membranes with large deformations in the absence of friction. The puncture strengths of elastomer membranes were found to be lower than their tensile and biaxial strengths. It was also found that the puncture of rubber membranes is controlled by a critical local deformation at the probe tip that is independent of the indentor geometry.

Furthermore, the puncture probes used in the ASTM F1342 standard and other available standard test methods are very different from real pointed objects like medical needles. In particular, their rounded tip does not bear the cutting edge of medical needles as illustrated in Figure 2.

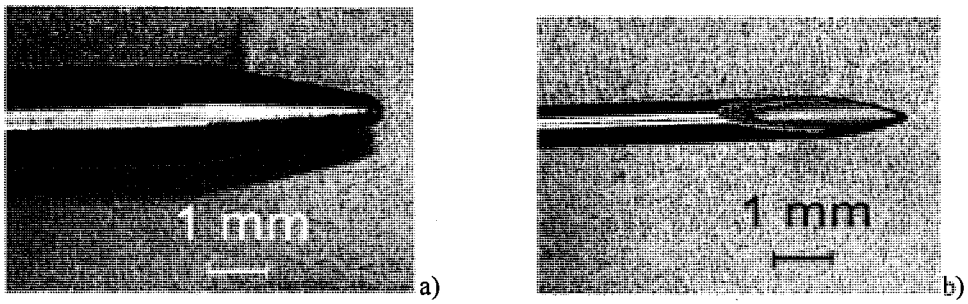

Fig. 2 a) Puncture probe A used in ASTM F1342 standard test; b) Medical needle

Results have also shown that the shape of the force-displacement curves recorded during puncture is very different for ASTM-type rounded probes and medical needles (Nguyen et al. 2005). While puncture by rounded probes occurs suddenly when the strain at the probe tip reaches the failure value, medical needles penetrate gradually through the sample. Puncture forces measured with medical needles have also been reported to be much smaller (Leslie et al. 1996; Hewett 1993; Dolez et al. 2008).

From a fundamental point of view, the puncture caused by sharp-pointed objects like medical needles is a complex phenomenon that may involve various fracture processes. For elastomer membranes tearing and cutting are the two major modes of failure that have been investigated. While tearing only involves the fracture energy of the material, both the fracture energy and the friction caused by the contact between the blade and the material contribute to cutting (Gent et al. 1994; Vu Thi et al. 2005). Based on the results obtained during a preliminary study carried out with neoprene, it was shown that puncture by medical needles seems to involve cutting, which is related to the material fracture energy (Nguyen et al. 2005). By comparison, puncture by ASTM-type rounded probes has been related to the material tension strength and failure strain. However, it must be noted that a large difference in geometrical configuration exists between cutting and needle puncture. Indeed, cutting involves a rectangular blade slicing through the whole sample thickness at the same time while moving along its length. On the other hand, needle puncture involves an elliptical sharp tip penetrating through the sample surface, into its thickness.

The aim of this work is to investigate the material parameters that control the puncture resistance of thin elastomer membranes to sharp-pointed objects like medical needles. In particular, the contributions of intrinsic material parameters to puncture by medical needles are verified. An approach is derived to compute the fracture energy associated to puncture by medical needles. The contribution of the friction energy to the calculated fracture energy is also discussed.

2. **Experimental**

Puncture tests were carried out on an Instron 1137 universal-testing machine. The puncture probes are held by a pin chuck mounted on a 167.7N load cell. A setup (see Fig. 3) comprising two steel plates bearing 10 mm holes is used to secure the elastomer samples. The edge of the hole in the lower plate is rounded to avoid stress concentration. All the tests were performed with a displacement rate of 50 mm/min unless specified otherwise. For each condition, a minimum of four replicates were produced.

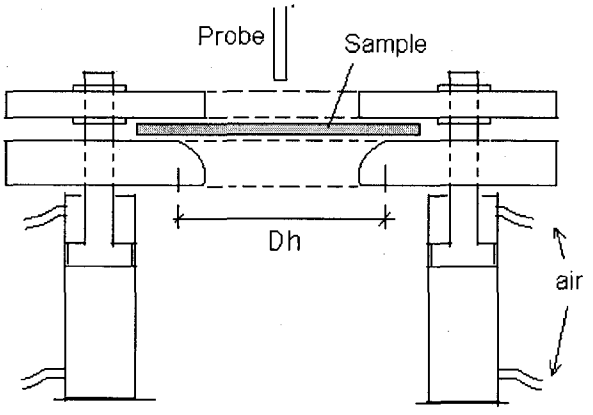

Fig. 3 Sample holder setup

In addition to the ASTM puncture probe A (see Figure 2a), a series of stainless steel medical needles obtained from PrecisionGlide^{TM} Pharma Co were used as puncture probes in this study. Their external diameter and tip angle measured as shown in Figure 4 are provided in Table 1.

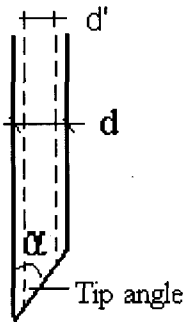

Fig. 4 Schematic representation of medical needles

Table 1: Medical needles used as puncture probes

Probe diameter: d (mm)	0.35	0.50	0.65
Probe tip angle: α	13.5°	11.2°	10.4°

Two types of commercial rubbers commonly used for protective gloves, neoprene and nitrile rubber, were investigated. Neoprene sheets with three different thicknesses, 0.40, 0.78 and 1.57 mm, were obtained from Fairprene Industrial Products. The nitrile rubber samples, 0.83 mm thick, were cut from nitrile rubber gloves manufactured by Ansell Co (glove model Sol-Vex 37-165).

Force-displacement data were recorded for the various puncture tests. Puncture force was measured as the maximum of the force-displacement curve. Needles were reused up to five times for puncture tests. Indeed, previous work has shown an increase in puncture force of less than 7% after ten successive uses of the same needle as puncture probe (Vu-Khanh et al. 2005).

3. Results and discussions

Puncture tests carried out with the ASTM puncture probe A and the medical needles were compared using the same thickness of neoprene. As shown in Figures 5 and 6 and in agreement to what has already been reported in the literature (Nguyen et al. 2005; Dolez et al. 2008), large differences can be observed in the shape of the force-displacement curve. For the rounded probes, puncture occurs instantly at maximum load (Figure 5); it has been associated to the point where the strain at the probe tip reaches the failure value (Nguyen et al. 2005). On the contrary, needles penetrate gradually through the sample thickness (Figure 6); after the force reaches a maximum, it diminishes slightly before reaching a plateau.

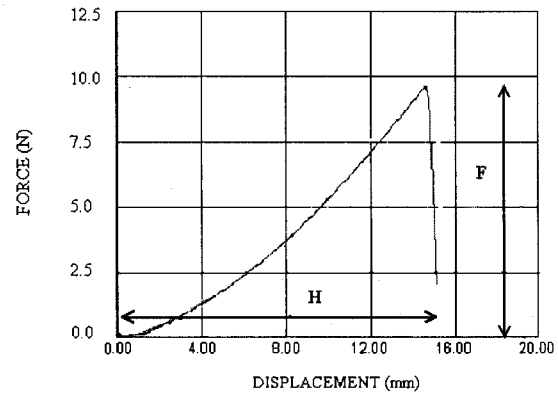

Fig. 5 Typical force - displacement curve for puncture with ASTM conical probe A (0.8-mm thick neoprene)

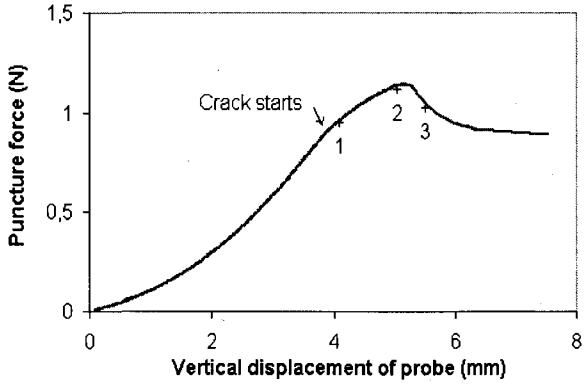

Fig. 6 Typical force - displacement for puncture with medical needles (0.8-mm thick neoprene, 0.5-mm diameter medical needle and 0.05 mm/min displacement rate)

In addition to the difference in the shape of the force-displacement curves, a strong reduction in the values of the maximum force and probe displacement at maximum force is observed with medical needles as illustrated in Table 2 for three thicknesses of neoprene.

Table 2: Puncture test results measured with ATSM puncture probe A and 0.5-mm diameter medical needles and three thicknesses of neoprene (coefficient of variation in parenthesis)

Sample thickness (mm)	0.40	0.78	1.57
ASTM F1342 conical probe A			
Puncture force (N)	5.1 (4%)	10.4 (3%)	19.2 (3%)
Probe displacement at puncture (mm)	14.7 (14%)	14.9 (12%)	15.3 (13%)
Medical needle 0.5 mm			
Puncture force (N)	0.5 (8%)	1.4 (7%)	2.2 (5%)
Probe displacement at puncture (mm)	2.7 (7%)	3.6 (6%)	5.3 (6%)

The very slow puncture speed (0.05 mm/min) used for Figure 6 allows a clear observation of the puncture process with medical needles. Before label 1 on the graph, the probe produces only a deformation of the sample. Label 1 indicates the point where the crack starts being initiated as illustrated in Fig. 7a. Between labels 1 and 2, the probe penetrates further into the sample thickness. At label 2, the probe has reached the bottom face of the sample, corresponding to the situation illustrated in the schematic in Fig. 7b.

When the needle tip emerges on the bottom surface of the membrane (label 3 on the graph in Fig. 6 and schematic in Fig. 7c), the needle tip can widen easily the punctured hole. As a consequence, the deformation of the sample under the needle tip is released and the whole

sample moves upward, with a decline in the force. The plateau observed in Fig. 6 at large displacements corresponds to the configuration where the cylindrical shaft of the needle is in contact with the sample. The measured force thus relates to the friction between the probe shaft and the puncture hole circumference.

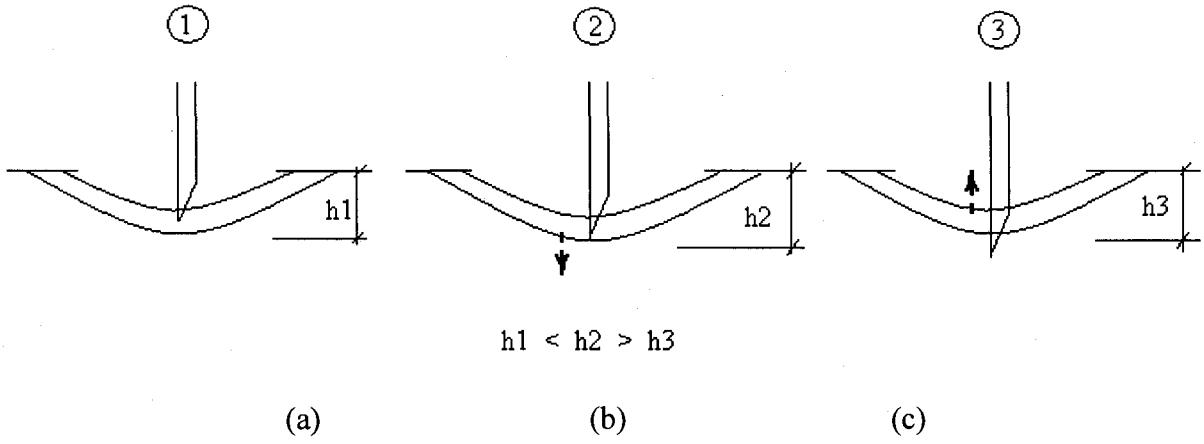

Fig. 7 Schematic representation of the sample deformation during the puncture process by medical needles

Figure 8 displays a zoom on the interval corresponding to the needle tip first penetration into the sample (i.e. between labels 1 and 2 in Fig. 6), with the probe displacement data converted to crack depth values (see insert in Fig. 8). It can be seen that, for neoprene, the puncture force varies linearly with crack depth. In addition, the slope is independent of the sample thickness on the studied range (between 0.4 and 1.5 mm).

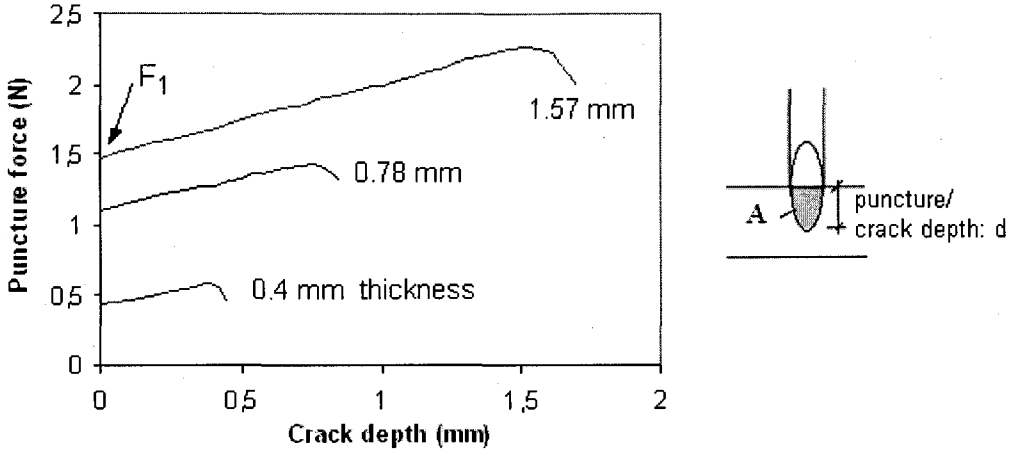

Fig. 8 Variation of the puncture force with crack depth for three thicknesses of neoprene (0.5-mm diameter medical needles)

In Figure 9, the force at crack start, i.e. at the point corresponding to label 1, is expressed as a function of the sample thickness in the case of neoprene. An increase in the force with the sample thickness can be observed. This result is interesting since at initiation, only the sample surface is penetrated and the contact force at the needle tip should be the same. Therefore it suggests that, in order for a crack to start, the local strain deformation of the sample around the needle tip must reach a critical value. For thicker samples, a larger force is needed to create the same level of deformation.

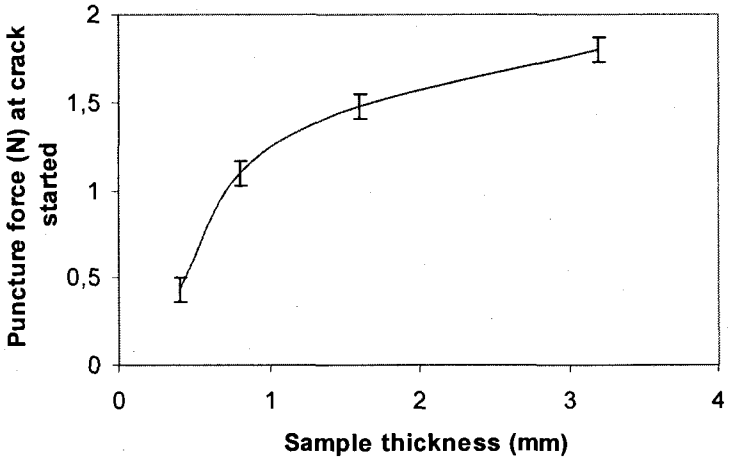

Fig. 9 Variation of the puncture force at crack start (F1) as a function of the sample thickness for neoprene (0.5-mm diameter medical needles)

Earlier studies have suggested that the puncture process associated with medical needles involves a cutting phenomenon (Nguyen et al. 2005). Other studies have related cutting to the fracture energy G_c of the material (Lake and Yeoh 1987; Cho and Lee 1998). According to the energy balance of fracture mechanics, the energy necessary to create a new fracture surface, the fracture energy G_s, can be expressed by (Felbeck and Atkins 1996):

$$G_s = -\left(\frac{\partial U}{\partial A}\right) \approx -\Delta U/\Delta A \qquad (1)$$

where ΔU is the change in strain energy corresponding to the change in fracture surface ΔA. For the case of needle puncture, the fracture surface created into the sample by medical needles is elliptical as shown in Figure 10.

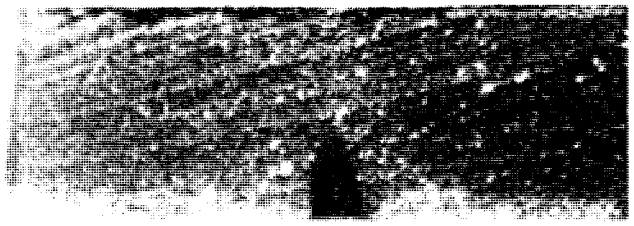

Fig. 10 Fracture surface created into a neoprene sample by a medical needle (optical microscopy: 20x)

ΔU can be measured from the loading curves: when the puncture has reached a certain depth into the sample, corresponding to a fracture surface A_i, the needle is withdrawn to get the return curve. Fig. 11 illustrates how the change in strain energy ΔU is computed by

subtracting the released energies corresponding to the different puncture depths. The changes in strain energy $-\Delta U_{ij}$ corresponding to the change of fracture surface ΔA_{ij} are thus:

$$-\Delta U_{ij} = U_i - U_j \ ;$$

$$\Delta A_{ij} = A_i - A_j \qquad (2)$$

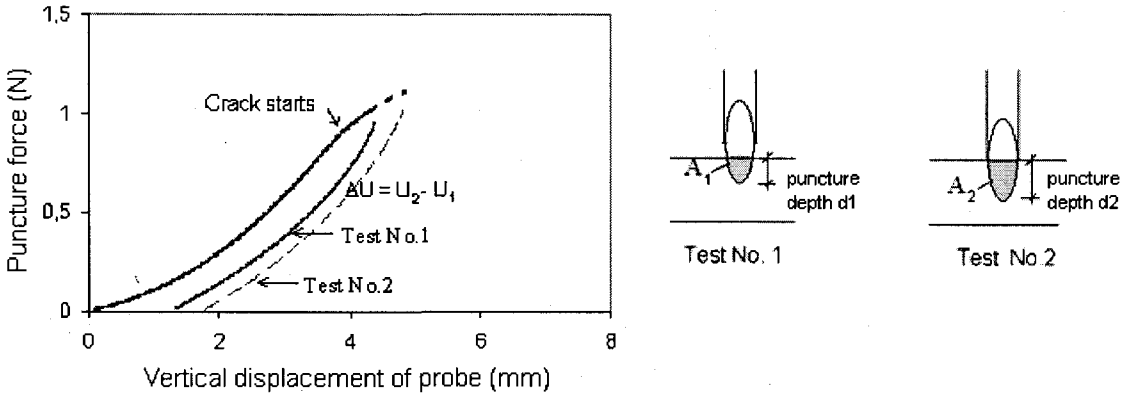

Fig. 11 Change in strain energy due to different puncture depths

Similar tests carried out on the same sample and with the same needle at different puncture depths provide different values of the released energy: $-U_1$, $-U_2$..., and the corresponding fracture surfaces: A_1, A_2... Fig. 12 displays the variation of the measured puncture energy G_s as a function of the puncture depth for different neoprene thicknesses. The results suggest a slight increase in G_s with the puncture depth, i.e. with puncture propagation.

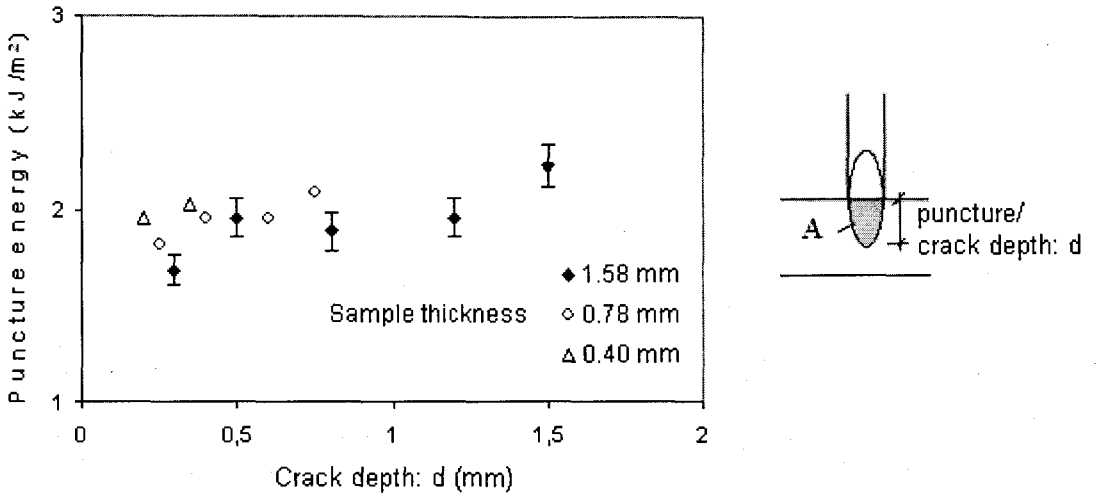

Fig. 12 Measured puncture energy as a function of crack depth for various thicknesses of neoprene and a 0.65-mm diameter medical needle.

A first approximation of the fracture energy at puncture initiation can be provided by the extrapolation at crack depth d = 0 of the measured puncture energies shown in Figure 12. This energy is displayed in Table 3 for three diameters of the medical needles and two thicknesses (0.40 and 1.57 mm) of neoprene. The results seem to suggest a constant value of puncture energy at initiation. However, a significant contribution of friction to the fracture energy has already been reported for cutting (Vu Thi et al. 2005).

Table 3: Extrapolated fracture energy of puncture for neoprene by medical needles (coefficient of variation in parenthesis)

Extrapolated fracture energy G_s (kJ/m^2)		Probe diameter: d (mm)		
		0.35	0.50	0.65
Sample thickness (mm)	0.40	1.7 (18%)	1.9 (14%)	1.8 (17%)
	1.57	1.8 (15%)	1.7 (14%)	1.7 (12%)

In order to verify the hypothesis of the friction contribution to the puncture energy, a BP™ lubricant was sprayed on the medical needles before their use as a puncture probe. Table 4 displays the results obtained in terms of extrapolated fracture energy both with and without lubricant for three medical needle diameters and two membrane materials, 1.57-mm thick neoprene and 0.83-mm thick nitrile rubber. The values of fracture energy seem to be slightly reduced by the use of the lubricant even if the difference is not statistically significant. In the case of nitrile rubber, the effect of friction does not appear to be totally removed by the use of lubricant as shown by the increasing values of the extrapolated fracture energy with the needle diameter.

Table 4: Extrapolated fracture energy for puncture by medical needles with and without lubricant (coefficient of variation in parenthesis)

Extrapolated fracture energy (kJ/m^2)		Probe diameter: d (mm)		
		0.35	0.50	0.65
Neoprene (1.57 mm)	Without lubricant	1.8 (15%)	1.7 (14%)	1.7 (12%)
	With lubricant	1.6 (13%)	1.6 (13%)	1.5 (11%)
Nitrile rubber (0.83 mm)	Without lubricant	3.8 (18%)	4.1 (14%)	4.2 (17%)
	With lubricant	3.6 (14%)	3.7 (13%)	4.0 (12%)

4. Conclusion

This work has demonstrated that the puncture by sharp-pointed objects like medical needles is very different from the puncture by conical probes like those used in the ASTM standard test for resistance to puncture. For elastomer materials, the puncture by conical probes is controlled by a local deformation or failure strain. On the other hand, for medical needles, the puncture process involves crack growth and fracture energy dissipation. A method based on the change in strain energy with the change in fracture surface is proposed for the characterization of the crack initiation energy due to puncture. However, even with the application of a lubricant on the needle surface, the effect of friction on the puncture process was not eliminated, preventing the determination of the material fracture energy.

Acknowledgements

This work has been supported in part by the Institut de recherche Robert-Sauvé en santé et en sécurité du travail.

References

- ASTM Standard F1342 (2005) Standard test method for protective clothing material resistance to puncture. In: ASTM International (ed) Annual Book of ASTM Standards, West Conshohocken, PA, vol 11.03, pp1489-1493
- Cho K, Lee D (1998) Viscoelastic effects in cutting of elastomers by a sharp object. J Polym Sci Part B: Polym Phys 36(8):1283-1291
- Dolez P, Vu-Khanh T, Nguyen C T, Guero G, Gauvin C, Lara J (2008) Influence of medical needle characteristics on the resistance to puncture of protective glove materials. J ASTM Int 5(1):12p
- Felbeck D K, Atkins A G (1996) Strength and Fracture of Engineering Solids. 2nd edn. Prentice-Hall Inc
- Gent A N, Lai S-M, Nah C, Wang C (1994) Viscoelastic effects in cutting and tearing rubber. Rubber Chem Technol 67(4):610–619
- Hewett D J (1993) Protocol for the puncture resistance of medical glove liners (personal communication)
- Lake G J, Yeoh O H (1987) Effect of crack tip sharpness on the strength of vulcanized rubbers. J Polym Sci 25:1157-1190
- Leslie L F, Woods J A, Thacker J G, Morgan R F, McGregor W, Edlich R F (1996) Needle puncture resistance of medical gloves, finger guards, and glove liners. J Biomedi Mater Research 33:41-46
- Nguyen C T, Vu-Khanh T (2004) Mechanics and mechanisms of puncture of elastomer membranes. J. Mater Sci 39(24):7361-7364
- Nguyen C T, Vu-Khanh T, Lara J (2004) Puncture characterization of rubber membranes. Theor Appl Fract Mech 42:25-33
- Nguyen C T, Vu-Khanh T, Lara J (2005) A Study on the puncture resistance of rubber materials used in protective clothing. J ASTM Int 2(4):245-258

- Vu-Khanh T, Vu Thi B N, Nguyen C T, Lara J (2005) Protective gloves: Study of the resistance of gloves to multiple mechanical aggressors. Rapport Études et Recherche R-424, Institut de recherche Robert-Sauvé en santé et en sécurité au travail, Montréal, QC, Canada, 74p
- Vu Thi B N, Vu-Khanh T, Lara J (2005) Effect of friction on cut resistance of polymers. J Thermoplast Compos Mat 18, n. 1, p. 23-36

CHAPTER 8: ARTICLE IV

PUNCTURE OF RUBBER MEMBRANES BY MEDICAL NEEDLES.

PART II: MECHANICS

Date d'acception: 12 Feb. 2009

État de l'acceptation: version finale publiée

Revue: *International Journal of Fracture - v.155 No.1 (2009) p.83-91*

1. C.Thang. Nguyen, étudiant au doctorat, Université de Sherbrooke, Faculté de génie, Département de génie mécanique
2. T. Vu-Khanh*, professeur, Université de Sherbrooke, Université du Québec / École de technologie supérieure, Département de génie mécanique
3. Patricia I. Dolez, Ph.D, Université de Sherbrooke, Université du Québec / École de technologie supérieure, Département de génie mécanique
4. Jaime Lara, Ph.D, Institut de recherche Robert-Sauvé en santé et en sécurité du travail, 505 de Maisonneuve Ouest, Montreal, QC, Canada, H3A 3C2

Référence : Nguyen C T, Vu-Khanh T, Dolez P I, Lara J (2009) *Puncture of elastomers membranes by medical needles. Part II: Mechanics.* International Journal of Fracture v.155 no.1: p.83-91

Titre français: Perforation de membranes élastomères par aiguilles médicaux. Partie II: Mécaniques

* toan.vu-khanh@etsmtl.ca

Abstract

Resistance to puncture by medical needles is becoming one of the most critical mechanical properties of rubber membranes, which are heavily used in protective gloves. Yet the intrinsic material parameters controlling the process of puncture by medical needles are still unknown. In a first paper presenting this two-part study, it has been shown that puncture by medical needles proceeds gradually as the needle cuts through the rubber membrane. The phenomenon of puncture by medical needles was revealed to involve contributions both from friction and fracture energy, in a similar way as for cutting. The use of a lubricant was not successful for removing the friction contribution for the determination of the material fracture energy corresponding to puncture by medical needles. This paper describes an alternative approach based on the application of a prestrain to the sample in a similar way as the work of Lake and Yeoh on cutting. A theoretical formulation for the tearing energy is derived from the theory of Rivlin and Thomas on the rupture of rubber. It is validated with a model extending expressions provided by the linear elastic fracture mechanics (LEFM) to include the non-linear stress-strain behavior displayed by rubber. For low values of the tearing energy, the total fracture energy, i.e. the sum of the puncture and tearing energies, is constant; the material fracture energy is obtained by extrapolation at zero tearing energy. This prestrain method allowed a complete removal of the friction contribution. The value obtained for the fracture energy corresponding to puncture by medical needles is found to be larger than the energy associated to cutting and smaller than that obtained for tearing. This can be related to the value of the crack tip diameter, which is, in that case, given by the needle cutting edge diameter.

Keywords:

Puncture, elastomers, medical needle, friction, fracture energy

1. Introduction

Medical needles have been more and more present as an occupational hazard, not only in health care but also for law enforcement and maintenance activities for example, with the associated risk of blood-borne pathogen transmission. Therefore, resistance to puncture by medical needles has become one of the most critical mechanical properties of rubber membranes, which are heavily used in protective gloves. Until now, only a very limited number of studies have dealt with puncture by medical needles. In some cases, they were evaluating new glove designs and materials (Leslie et al. 1996; Edlich et al. 2003a; Edlich 2003b). Others were looking into the effect of experimental parameters like needle characteristics (Hewett 1993; Dolez et al. 2008). However, the intrinsic material parameters controlling the process of puncture by medical needles are still unknown, which limits the ability to improve the level of protection available for workers.

A few fundamental investigations on puncture have been carried out using round and flat geometries for the probe tip. In a study involving cylindrical indentors and rubber blocks, it has been shown that a ring-shaped starter crack is created on the block surface before puncture occurs (Stevenson and Kamarudin 1994). For flat indentors, the value of the measured fracture energy associated with puncture agrees well with the energy obtained from catastrophic tearing. For elastomer membranes, other studies using flat, spherical and conical probes revealed that the probe tip geometry strongly affects the puncture force in elastomers (Nguyen et al. 2004; Ngyuen and Vu-Khanh 2004); the maximum puncture force depends on the contact surface between the membrane and the probe tip. Using the Mooney strain-energy function, the indentation force was calculated for elastomer membranes with large deformations. The results showed that the puncture of rubber membranes is in fact controlled by a critical local deformation at the probe tip that is independent of the indentor geometry.

In the case of medical needles, the presence of a cutting edge (see Fig. 1) leads to a different mechanism. Preliminary works have shown that the shape of the force-displacement curves recorded during puncture is very different for flat or rounded probes and medical needles (Nguyen et al. 2005). While in the first case, puncture occurs suddenly when the strain at the

probe tip reaches the failure value, medical needles penetrate gradually through the sample. Puncture forces measured with medical needles have also been found to be much smaller (Leslie et al. 1996; Hewett 1993, Dolez et al. 2008).

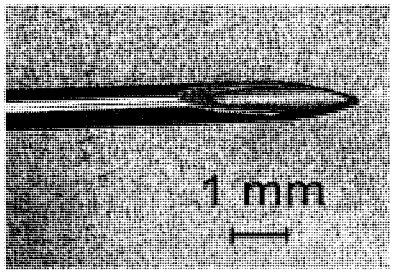

Fig. 1 Medical needle

In addition, results provided in the first paper of this two-part study have shown that for medical needles, the puncture process involves both cutting and fracture energy (Nguyen et al. submitted). A method based on the change in strain energy with the change in fracture surface was developed for the computation of the fracture energy due to puncture. A lubricant was applied on the needle to try to limit the effect of friction. However, the results showed that the friction contribution was not eliminated.

This paper investigates an alternative method for removing the friction contribution from the total fracture energy associated with puncture by medical needles. It is based on the application of a prestrain on the sample, which moves the sample fracture surfaces apart from the probe body and limits the contact only to the probe tip. This technique has been used by researchers who combined tearing and cutting or puncture to get access to the exact value of the material fracture energy (Lake and Yeoh 1978; Lake and Yeoh 1987; Gent et al. 1994; Cho and Lee 1998). In particular, Lake and Yeoh proposed a test method to evaluate the cutting energy of rubbers in which the frictional contribution was excluded by pre-straining the sample before forcing a razor blade into a crack tip (Lake and Yeoh 1978; Lake and Yeoh 1987). While cutting is induced by a rectangular blade slicing through the whole sample thickness and moving along its length, puncture is made by pushing the needle with an

elliptical sharp tip penetrating through the sample surface, into its thickness, and tearing involves the propagation of a crack under tensile loading of a pre-notched sample.

Since puncture by medical needles has been shown to involve friction, the same principles are used to try to eliminate friction from the puncture process and thus get access to the true material fracture energy associated with puncture of elastomer membranes by medical needles. The theoretical treatment involves the determination of the tearing energy, which is derived both from the theory of Rivlin and Thomas on the rupture of rubber (Rivlin and Thomas 1953) and from an extension of expressions provided by the linear elastic fracture mechanics (LEFM) (Felbeck and Atkins 1996) to the case of non-linear stress-strain behavior displayed by rubber. The complete removal of the friction contribution from the measurement of the fracture energy is further verified by application of a lubricant to the needle surface.

2. Experimental

A special set-up was designed to apply a prestrain to the sample while it is punctured by a medical needle, as illustrated in Figure 2. The sample is extended along its length and a puncture force is applied in the direction of its thickness, i.e. perpendicular to the prestrain. As already mentioned by Lake and Yeoh (Lake and Yeoh 1978; Lake and Yeoh 1987), this configuration may cause an out-of-plane effect. However, it must be minor since puncture forces are more than an order of magnitude smaller than the applied prestrains (1-2 N for the puncture force compared to 20-40 N for the prestrain force).

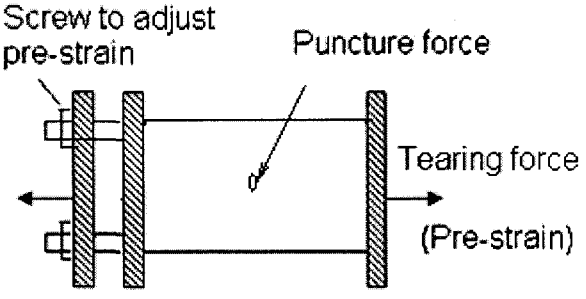

Fig. 2 Schematic representation of the sample holder designed for applying a prestrain on samples being subjected to puncture by medical needles

The puncture tests with prestrained samples were performed in an Instron 1137 universal-testing machine. A complete description of the testing configuration can be found in the first part of this work (Nguyen et al. submitted). Medical needles from PrecisionGlide^{TM} Pharma Co with a diameter of 0.65 mm were used as puncture probes. All the tests were performed with a displacement rate of 50 mm/min. For each condition, a minimum of four replicates were produced.

Two types of commercial rubbers commonly used for protective gloves, neoprene and nitrile rubber, were investigated. Neoprene sheets, 1.6 mm in thickness, were obtained from Fairprene Industrial Products. Nitrile rubber samples, 0.8-mm thick, were cut from nitrile rubber gloves manufactured by Ansell Co (glove model Sol-Vex 37-165).

The force-displacement data were recorded for the various puncture test conditions. The puncture force was measured at the maximum of the force-displacement curve. Needles were reused up to five times for puncture tests. Indeed, previous work has shown an increase in puncture force of less than 7% after ten successive uses of the same needle as puncture probe (Vu-Khanh et al. 2005).

3. Results and discussions

Figure 3 illustrates the effects of prestrain on the variation of the puncture force as a function of the puncture probe displacement. While the general shape of the curve is preserved, the values of the maximum puncture force as well as the probe displacement are reduced with increasing values of the prestrain. In addition, the feature associated with the point where the crack starts being initiated (the shoulder in the right side of the curve (Nguyen et al. submitted)) is amplified by the application of a prestrain.

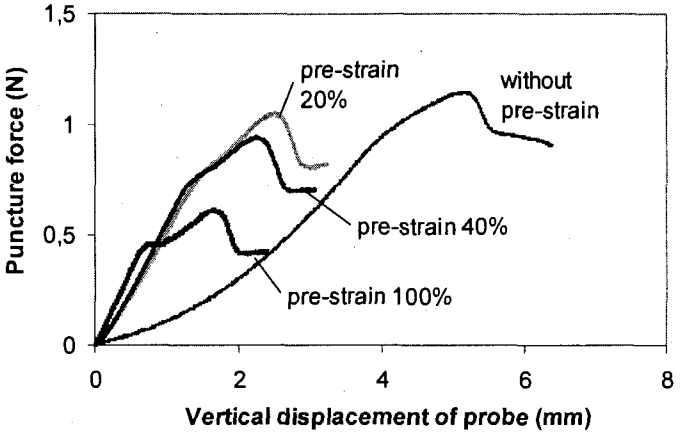

Fig. 3 Typical force - displacement curves at different prestrain levels (neoprene)

A technique has been developed for evaluating the fracture energy associated to puncture (Nguyen et al. submitted). It is based on the change in strain energy with puncture depth. The strain energy release rate is calculated as the area delimited between the puncture and the return curve (when the needle is withdrawn). The fracture surface was measured by optical microscopy. The fracture energy G_s is given by:

$$G_s = -\left(\frac{\partial U}{\partial A}\right) \approx -\frac{\Delta U}{\Delta A} \tag{1}$$

where ΔU is the change in strain energy corresponding to the change in fracture surface ΔA.

The same technique was used for the calculation of the puncture energy with an applied prestrain. Figure 4 displays the variation of the calculated puncture energy as a function of the crack depth for different values of the pre-strain in the case of the 1.6-mm thick neoprene membrane and 0.65-mm diameter medical needles. The increase in puncture energy with

crack depth, observed for non-prestrained samples, was attributed to the effect of friction between the membrane fracture surface and the needle (Nguyen et al. submitted). This effect disappears with the use of a prestrain larger than 20%.

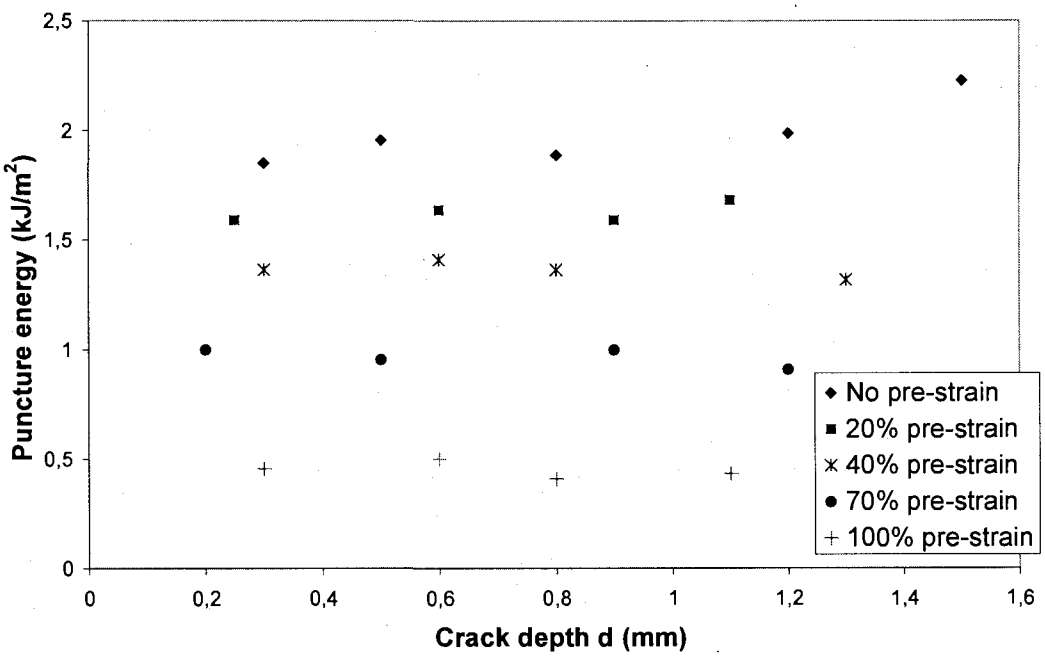

Fig. 4 Puncture energy as a function of crack depth for neoprene at different pre-strain levels

Extending the principles proposed by Lake and Yeoh (Lake and Yeoh 1978; Lake and Yeoh 1987) to this case combining puncture and tearing, the total energy G corresponding to a unit increase in the fracture surface area is provided by:

$$G = T + P \qquad (2)$$

with P the puncture energy and T the prestrain or tearing energy. Following what has been obtained by Lake and Yeoh for cutting, the total fracture energy G, which depends only on the

tested material and probe sharpness (Lake and Yeoh 1978), should be constant in the low tearing energy region, i.e. an increase in the tearing energy T should correspond to a decrease in the puncture energy P, which has been associated with true cutting. A more complex behavior involving tearing is expected at higher tearing energies.

In order to evaluate the tearing energy T, a theoretical model has been developed based on the work of Rivlin and Thomas on cutting (Rivlin and Thomas 1953). They showed that when a small cut is made in a test piece stretched in simple extension, the change in the total stored energy in the test piece is given by:

$$W_t - W = \beta c^2 t S_e \qquad (3)$$

where W_t and W are the total stored energies before and after the cut is made. $2c$ and t are, respectively, the length of the cut and the thickness of the test piece measured in the undeformed state (see Figure 5). S_e is the stored-energy density corresponding to the extension ratio λ in the simple extension region and β is a numerical factor that varies with λ. When expressed as a function of the fracture surface A ($A = 2ct$), equation (3) becomes:

$$W_t - W = \frac{\beta A^2 S_e}{4t} \qquad (4)$$

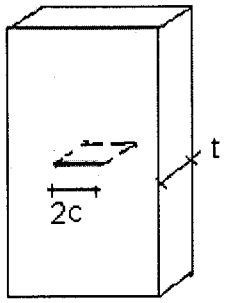

Fig. 5 Crack geometry for cutting (corresponding to the Rivlin and Thomas description)

Rivlin and Thomas (Rivlin and Thomas 1953) and Greensmith (Greensmith 1963) determined that β decreases from a value of 3 at low extension to a value close to 2 at $\lambda = 3$. They also showed that the change in the elastically stored energy S_e value due to the presence of the cut is only minor (a few %). Consequently, S_e can be expressed as a function of λ by (Rivlin and Thomas 1953):

$$S_e = C_1\left(\lambda^2 + \frac{2}{\lambda} - 3\right) + C_2\left(\frac{1}{\lambda^2} + 2\lambda - 3\right) \tag{5}$$

in which C_1 and C_2 are the Mooney-Rivlin coefficients determined from tensile tests and λ is the extension ratio of the prestrained test piece.

Using Eq. 4, the tearing energy T can be calculated as:

$$T = -\left(\frac{\partial W}{\partial A}\right) = \frac{\partial(\beta A^2 S_e/4t)}{\partial A} = \frac{2\beta A S_e}{4t} = \frac{1}{2}\beta c S_e \tag{6}$$

For the case of puncture tests on pre-strained samples, the same principle can be used while taking into account the difference in the crack geometry, as illustrated in Fig. 5 and Fig. 6. In the case of puncture, the crack has the eliptical shape of the needle tip. The crack surface area A is thus equal to:

$$A = \pi cd/2 \tag{7}$$

With d the puncture depth and $2c$ the cut length created by the puncture probe (see Fig. 6).

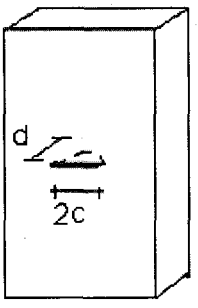

Fig. 6 Crack geometry for puncture

In addition, the crack does not go through the whole sample thickness. As a consequence, Eq. 3 has to be rewritten as:

$$W_t - W = \beta d^2 c S_e = \frac{4\beta A^2 S_e}{\pi^2 c} \tag{8}$$

Using the same considerations as for the determination of Eq. 6, the tearing energy for puncture is given by the following relationship:

$$T = -\left(\frac{\partial W}{\partial A}\right) = \frac{4}{\pi}\beta\, d\, S_e \tag{9}$$

The determination of the numerical factor $\beta(\lambda)$ can be carried out by adapting the method developed by Greensmith (Greensmith 1963), which is based on the measurement of the elastic properties of rubber. According to Eq. 8, β is provided by:

$$\beta = \frac{W_t - W}{d^2\, c\, S_e} \tag{10}$$

In the case of a partial pre-cut performed with a medical needle in a sample subjected to simple tension, the change in the sample total energy is given by:

$$W_t - W = \int_{lo}^{l} (F_t - F)\, dl \tag{11}$$

With F_t, the force on the sample in the absence of a cut, and F, the force in the presence of a pre-cut of length $2c$ and depth d.

When expressed as a function of the extension ratio $\lambda = l/l_o$, Eq. 11 becomes:

$$W_t - W = \int_{1}^{\lambda} l_0 (F_t - F)\, d\lambda \tag{12}$$

The stored-energy density S_e can be calculated according to (Rivlin and Thomas 1953):

$$S_e = \int_1^{\lambda} (F_t / A_0)\, d\lambda \tag{13}$$

By combining Eqs. 10, 12 and 13, β is given by:

$$\beta = \frac{\int_1^{\lambda} \left[l_o (F_t - F) / d^2 c \right] d\lambda}{\int_1^{\lambda} (F_t / A_o)\, d\lambda} \tag{14}$$

Values of $[l_o(F_t - F)/d^2c]$ can be extracted from the stress-strain curves obtained for neoprene samples with and without pre-cut (see Fig. 7). They are plotted together with the values of the total stress F_t/A_o as a function of the extention ratio λ in Fig. 8.

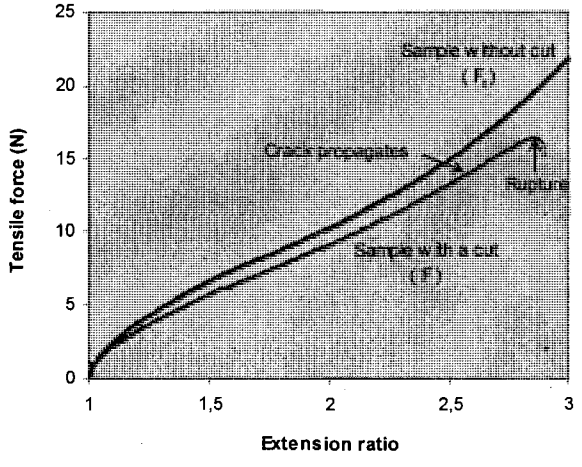

Fig. 7 Stress-strain curves for neoprene with and without pre-cut (pre-cut done with a 0.65-mm diameter needle)

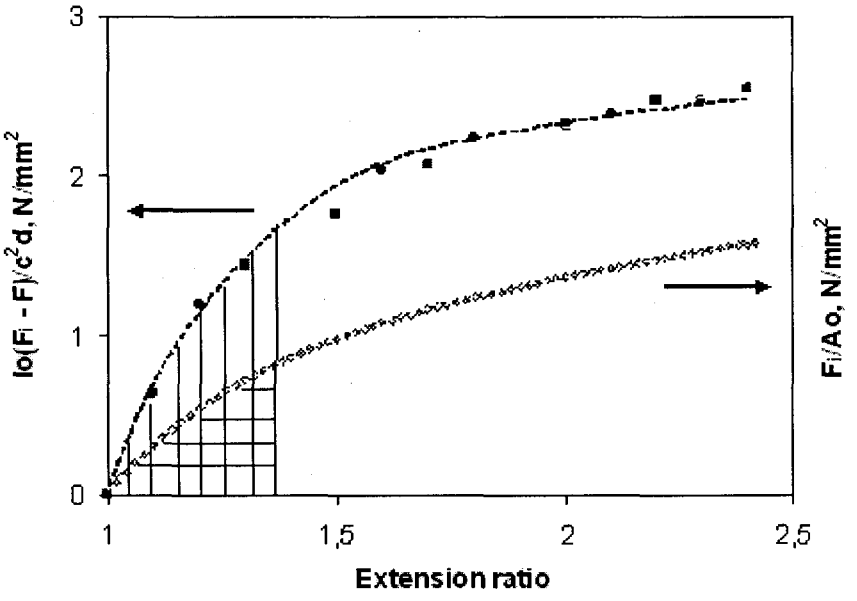

Fig. 8 Values of $l_o(F_t - F)/d^2c$ and F_t/A_o displayed as a function of the extention ratio λ

According to Eq. 14, β is given by the ratio of the areas under the two curves displayed in Fig. 8. Fig. 9 displays the variation of β as a function of the extension ratio calculated using this method for neoprene and nitrile rubber.

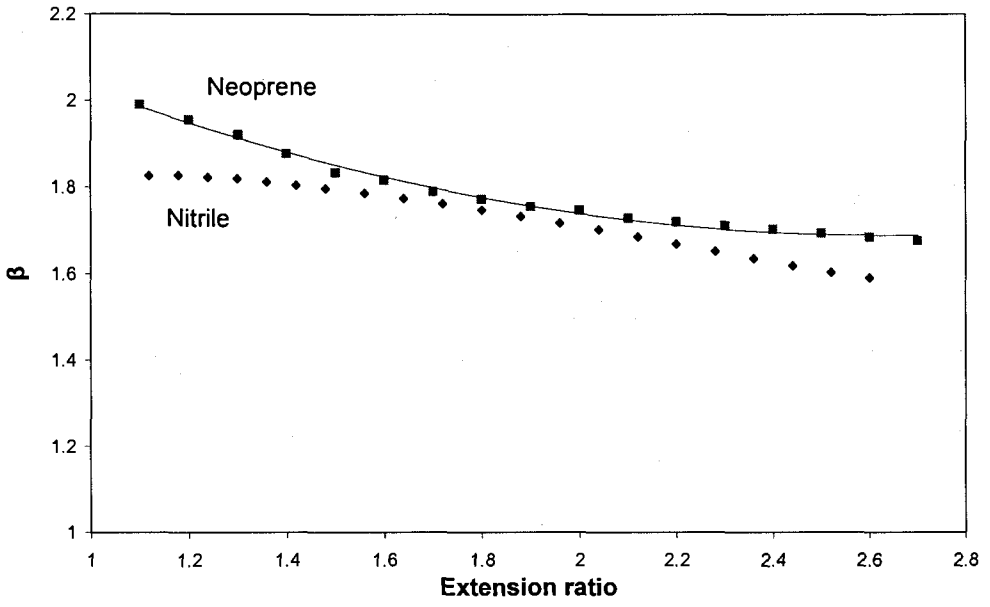

Fig. 9 Variation of β as a function of the extention ratio λ for neoprene and nitrile rubber calculated using Eq. 14

Using the data for β displayed in Fig. 9 and the values of the Mooney-Rivlin coefficients provided from tensile tests (Eq. 5), the tearing energy T can be computed according to Eq. 9. Figure 10 displays the variation of the tearing energy for 1.6-mm thick neoprene (C_1 = 172 kPa, C_2 = 443 kPa) as a function of the extension ratio or prestrain.

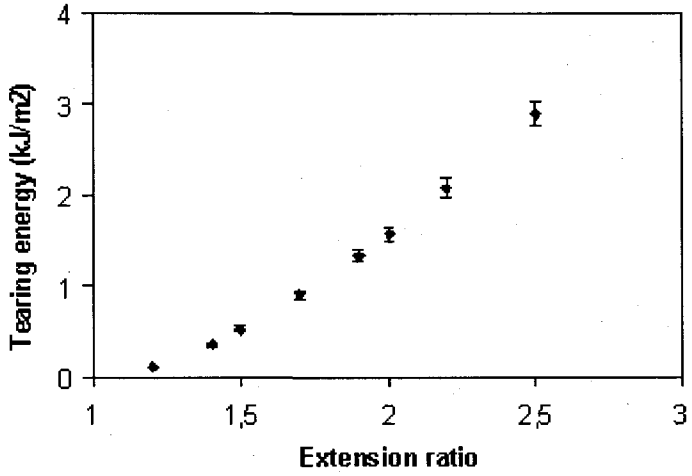

Fig. 10 Variation of the tearing energy as a function of the extension ratio for 1.6-mm thick neoprene (C_1 = 172 kPa, C_2 = 443 kPa) computed using Eq. 9

To further verify the computation of the tearing energy T described above, an alternative method has been developed: the linear elastic fracture mechanics (LEFM) is applied to rubber by taking into account its non-linear stress-strain behavior. More specifically, it consists in i) replacing the stored-energy density $\sigma^2/2E$ in LEFM by $S_e(\lambda)$ provided by Eq. 5, and ii) using the expressions $c = c_o/\lambda^{1/2}$ and $d = d_o/\lambda^{1/2}$ respectively for the crack length and the crack depth (c_o and d_o in the unstrained state) in order to take into account the shortening of the crack with the extension ratio λ.

For an elliptical crack when applied to rubber and for the case d>c, the stress intensity factor K in LEFM is given by (Felbeck and Atkins 1996):

$$K = 1.12\frac{\sigma}{\Phi}\sqrt{\pi d^2 / c} \tag{15}$$

with Φ a numerical factor, which is provided by the following relationship:

$$\Phi = \frac{3\pi}{8} + \frac{\pi}{8}\frac{d^2}{c^2} \tag{16}$$

The expression for the tearing energy T from the LEFM becomes:

$$T = \frac{K^2}{E} = Y\frac{\sigma^2}{E}\frac{d^2}{c} = \frac{2YS_e}{\lambda^{1/2}}\frac{d^2}{c} \tag{17}$$

with Y a geometry factor ($Y = 1.254\pi/\Phi^2$ (Felbeck and Atkins 1996)).

The results obtained for the tearing energy as a function of the extension ratio or prestrain using both methods, i.e. the Rivlin and Thomas formalism (Eq. 9) and the extension to rubber of the LEFM principles (Eq. 17), are compared in Fig. 11 in the case of 1.6-mm thick neoprene. Even if the calculation represented by Eq. 17 is simple, it agrees well with the more complex method based on the Rivlin and Thomas formalism.

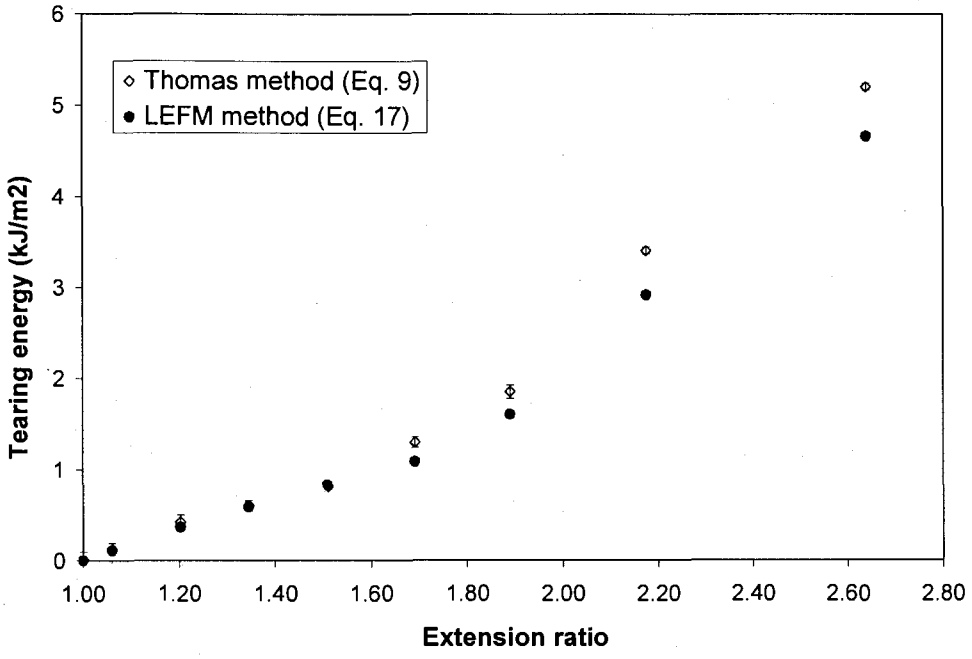

Fig. 11 Comparison of the calculation of the tearing energy T using Eq. 9 (method based on the Rivlin and Thomas theory) and Eq. 17 (LEFM extended to rubber) for 1.6-mm thick neoprene

Using Eq. 9 and 17 for the calculation of the tearing energy corresponding to the different values of applied prestrain, it is possible to express the data of Fig. 4 for neoprene in terms of the variation of the puncture energy as a function of the tearing energy. They are displayed in Fig. 12. A good agreement is obtained between the curves calculated using the Rivlin and Thomas and the LEFM methods. This demonstrates the validity of the approximations made in the computation of Eq. 17 using the LEFM extended to rubber.

A linear region can be observed at the low values of the tearing energy, corresponding to a constant value of the total energy G corresponding to a unit increase in fracture surface area (Eq. 2). At high tearing energies, puncture contributes only to the initiation of the crack, which propagates under the sole effect of the tearing energy. In that case, the contribution of puncture is only marginal. This result indicates that the same principle used by Lake and

Yoeh for cutting applies to the case of puncture by needles. As a consequence, the fracture energy associated to puncture can be calculated by extrapolating the linear part of the curve in Fig. 12 to zero tearing energy.

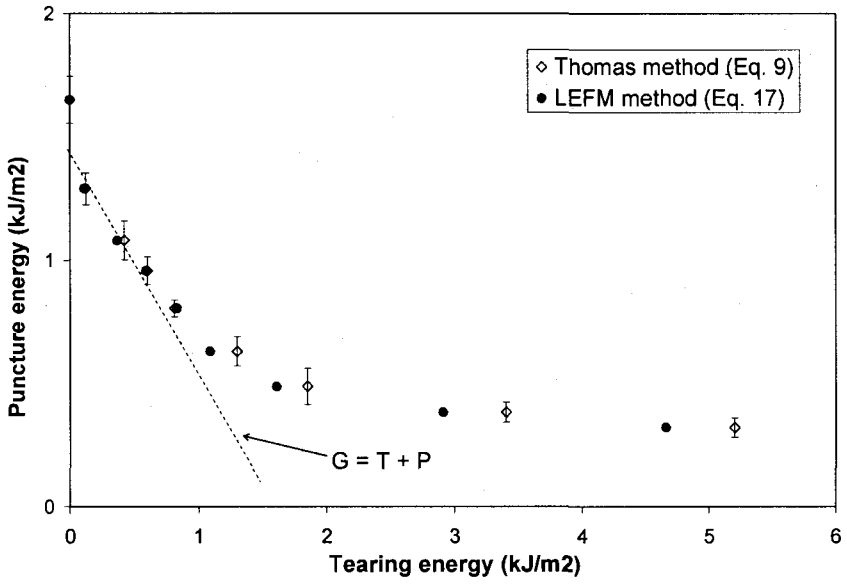

Fig. 12 Variation of the puncture energy with tearing energy calculated using Eq. 9 (method based on the Rivlin and Thomas theory) and Eq. 17 (LEFM extended to rubber) for 1.6-mm thick neoprene

In order to verify that all friction has been removed by the use of this prestrain technique, tests were performed with combining the application of the prestrain on the sample and of a lubricant on the surface of the needle. Fig. 13 displays a comparison of the variation of the puncture energy as a function of the tearing energy for the case of nitrile rubber with and without the application of the lubricant on the needle. In the linear region and for large tearing energies, data points superimpose, which indicates that no further reduction of the friction is brought by the lubricant. On the other side, in the zero or very low tearing energy region, a small difference seems observable, considering the uncertainty in measurement. It could be attributed to the fact that, in that case, the tearing energy is not large enough to

eliminate all the influence of the friction. These results suggest that the prestrain technique allows complete removal of friction contribution for the determination of the fracture energy associated to puncture.

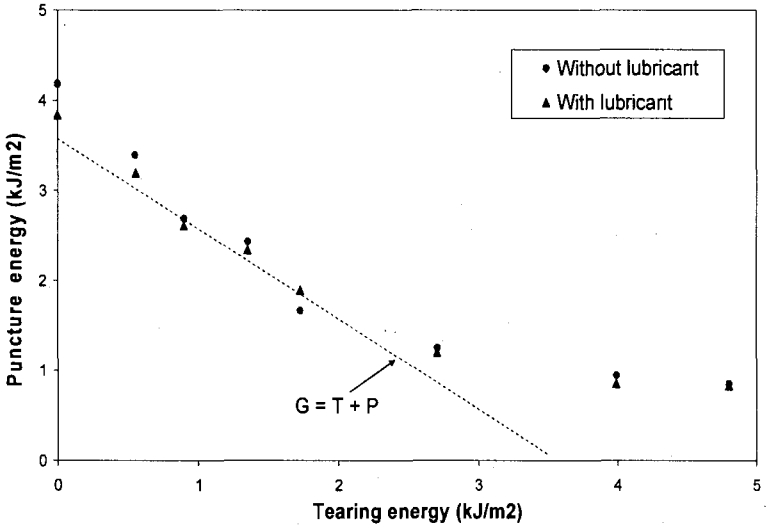

Fig. 13 Variation of the puncture energy with tearing energy for 0.8mm-thick nitrile rubber

Values of the fracture energy associated with puncture by medical needles were calculated for neoprene and nitrile rubber using the prestrain technique and the extrapolation to zero prestrain. They are displayed in Table 1. Also provided in this table are the values of fracture energy for cutting and tearing reported for the same neoprene (Ha Anh and Vu-Khanh 2004) and the same nitrile rubber (Vu Thi 2004) as the ones used in this study. In these experiments, the cutting fracture energy was measured using the stretched Y-shaped set-up and the tearing energy was provided by trouser tests.

Table 1 Values of fracture energy associated with puncture by medical needles (0.65-mm diameter), cutting and tearing for neoprene and nitrile rubber

	Neoprene (1.6-mm thick)	Nitrile rubber (0.8-mm thick)
Fracture energy for puncture by medical needles (kJ/m^2)	1.52	3.54
Fracture energy for cutting (kJ/m^2)	0.7*	1.38[#]
Fracture energy for tearing (kJ/m^2)	6.2*	9.6[#]

* from (Ha Anh and Vu-Khanh 2004); [#] from (Vu Thi 2004)

The fracture energy for puncture by medical needles is observed to be larger than that associated with cutting and smaller than that relative to tearing. This can be explained by considering the work of Thomas on rubber fracture (Thomas 1955). He found that the energy release rate during fracture is closely related to the strain energy density in the material at the tip (where fracture occurs). He proposed a relationship of the form:

$$G = W_t \, d \tag{18}$$

where W_t is the average energy density at the tip and d is the effective tip diameter. The validity of Eq. 18 was verified by direct and photoelastic measurements of the strain energy distribution around a model crack tip (Thomas 1955; Andrews 1961). A good agreement was obtained between the tearing energy determined by this way and the value calculated from the applied forces. In addition, tear experiments involving tip diameters between 0.1 to 3 mm provided consistent values of the tearing energy T, with W_t (derived from Eq. 18) being similar to the work to break measured independently from a tensile test (Thomas 1955).

The crack tip diameter in cutting for rubbers has been found to be controlled by the blade edge radius, about 0.05 μm (Gent et al. 1994; Cho and Lee 1998). In particular, it was shown that the cutting energy is much higher than the threshold fracture energy, even in the threshold condition of cutting process, due to a restriction in the change of the crack tip diameter by the razor blade (Cho and Lee 1998). At threshold conditions, i.e., at low speeds and high temperatures, the crack tip for cutting remains blunt; the roughness of the fracture surface is attributed to the roughness of the blade tip. On the other side, the dimension of the crack tip associated to rubber tearing is much larger, especially when blunting occurs. It has been estimated to lie in the range of 0.1 to 1 mm (Gent et al. 1994).

For the case of medical needles, it can be assumed that the crack tip radius is also controlled by the sharpness of the needle penetrating edge. The latter therefore depends on a number of manufacturing characteristics, in particular the facet angle, the number of facets, etc. In the case of the medical needles used in this study, from optical microscopic observation, we have estimated that it is much larger than the blade edge radius involved in cutting and smaller than the crack tip radius created by tearing. This difference in crack tip radius may thus explain the difference in fracture energy for puncture by medical needles, cutting and tearing for neoprene and nitrile rubber shown in Table 1.

4. Conclusion

In the continuation of the work reported in a first paper dealing with the mechanisms of puncture of elastomer membranes by medical needles, this paper has described the method used to measure the fracture energy associated with puncture by medical needles. The contribution of friction to the puncture energy was successfully completely removed by the application of a prestrain, in a similar way to what had been developed by Lake and Yeoh for cutting. The theoretical formulation allowing the calculation of the tearing energy associated to this applied prestrain was derived from the theory of Rivlin and Thomas on the rupture of rubber. It was validated with a model extending expressions provided by the linear elastic

fracture mechanics (LEFM) to include the non-linear stress-strain behavior displayed by rubber.

Values for the fracture energy corresponding to puncture by medical needles have been obtained for neoprene and nitrile rubber. They are found to be larger than the energy associated to cutting and smaller than that obtained for tearing. This can be related to the value of the crack tip diameter, which is, in that case, controlled by the needle cutting edge diameter, and is much larger than blade edge diameters and smaller than the crack tip dimension associated with tearing in rubbers.

Acknowledgements

This work has been supported in part by the Institut de recherche Robert-Sauvé en santé et en sécurité du travail.

References

- Andrews A G (1961) Stresses at crack in elastomer. Proc Phys Soc 77(494):483-498
- Cho K, Lee D (1998) Viscoelastic effects in cutting of elastomers by a sharp object. J Polym Sci Part B: Polym Phys 36(8):1283-1291
- Dolez P, Vu-Khanh T, Nguyen C T, Guero G, Gauvin C, Lara J (2008) Influence of medical needle characteristics on the resistance to puncture of protective glove materials. J ASTM Int 5(1):12p
- Edlich R F, Wind T C et al (2003a) Reliability and performance of innovative surgical double-glove hole puncture indication systems. J Long-Term Eff Med Implants 13(2):69-83
- Edlich R F, Wind T C et al (2003b). Resistance of double-glove hole puncture indication systems to surgical needle puncture. J Long-Term Eff Med Implants 13(2):85-90
- Felbeck D K, Atkins A G (1996) Strength and Fracture of Engineering Solids. 2nd edn. Prentice-Hall Inc
- Gent A N, Lai S-M, Nah C, Wang C (1994) Viscoelastic effects in cutting and tearing rubber. Rubber Chem Technol 67(4):610–619
- Greensmith H W (1963) Rupture of rubber: X. The change in stored energy on making a small cut in a test piece held in simple extension. J Appl Polym Sci 7:993-1002
- Ha-Anh T, Vu-Khanh T (2004) Thermoxidative aging effect on mechanical performances of polychloroprene. J Chin Inst Eng 27(6):753-761
- Hewett D J (1993) Protocol for the puncture resistance of medical glove liners (personal communication)
- Leslie L F, Woods J A, Thacker J G, Morgan R F, McGregor W, Edlich R F (1996) Needle puncture resistance of medical gloves, finger guards, and glove liners. J Biomedi Mater Research 33:41-46
- Lake G H, Yeoh O H (1978) Measurement of rubber cutting resistance in the absence of friction. Inter J Fract 14(5):509-526
- Lake G J, Yeoh O H (1987) Effect of crack tip sharpness on the strength of vulcanized rubbers. J Polym Sci 25:1157-1190
- Nguyen C T, Vu-Khanh T (2004) Mechanics and mechanisms of puncture of elastomer membranes. J. Mater Sci 39(24):7361-7364
- Nguyen C T, Vu-Khanh T, Lara J (2004) Puncture characterization of rubber membranes. Theor Appl Fract Mech 42:25-33
- Nguyen C T, Vu-Khanh T, Lara J (2005) A Study on the puncture resistance of rubber materials used in protective clothing. J ASTM Int 2(4):245-258

- Nguyen C T, Vu-Khanh T, Dolez P I, Lara J (2009) Puncture of elastomers membranes by medical needles. Part I: Mechanisms. Inter J Fract
- Rivlin R S, Thomas A G (1953) Rupture of rubber: I. Characteristic energy for tearing. J Polym Sci 10(3):291-318
- Stevenson A, Malek K A (1994) On the puncture mechanics of rubber. Rubber Chem Technol 67(5):743-760
- Thomas A G (1955) Rupture of rubber: II. The strain concentration at an inclusion. J Polym Sci 18:177-188
- Vu-Khanh T, Vu Thi B N, Nguyen C T, Lara J (2005) Protective gloves: Study of the resistance of gloves to multiple mechanical aggressors. Rapport Études et Recherche R-424, Institut de recherche Robert-Sauvé en santé et en sécurité au travail, Montréal, QC, Canada, 74p
- Vu Thi B N (2004) Mécanique et mécanisme de la coupure des matériaux de protection. Ph.D. dissertation, Université de Sherbrooke (QC, Canada)

CHAPTER 9

CONCLUSIONS

The results in this work show that the puncture of the elastomer membrane with the probes used in the F1342 ASTM standard is controlled by a local deformation that is an intrinsic material parameter, and is independent of the indentor geometry. The puncture strength is much smaller than both the tensile and the biaxial stresses. The maximum stress in puncture corresponds to the maximum strains measured from the top surface of the probe.

The results of puncture by cylindrical probes are useful for the characterization of the puncture resistance of elastomeric membranes. Indeed, a simpler cylindrical probe can be used in the place of the costly conical probe required by the ASTM Standard and still provides a quantitative characterization of puncture. Furthermore, the rounded-tip probe gives exactly the same result as that of the flat-tip probe. Since the cylindrical probe is much easier to produce, the expensive ASTM probe can be replaced by a simple cylindrical probe.

Furthermore, it has been demonstrated in this work that the puncture of sharp-pointed objects (medical needles) is very different from the puncture of conical probe in the ASTM F1342. In fact, puncture by medical needles is shown to proceed gradually as the needle cuts into the membrane. This behavior is highly different from puncture by rounded probes which occurs suddenly when the strain at the probe tip reaches the failure value. In addition, maximum force values are observed to be much smaller with medical needles. For medical needles, the puncture resistance involves cutting and fracture energy of material. A method has been developed based on the change in strain energy with the puncture depth to evaluate the fracture energy associated with puncture. The results show that the phenomenon of puncture by medical needles involves contributions both from friction and fracture energy, in a similar way as for cutting. A lubricant was tentatively used to reduce the friction contribution for the computation of the material fracture energy.

However, the lubricant can not eliminate totally the friction which is dependent on the material and lubricant type. Therefore, a method which is similar of Lake and Yeoh for cutting, is also described to assess the fracture energy in puncture of rubbers by sharp-pointed

objects. The method enables the effects of friction on the evaluation of fracture energy in the puncture process to be substantially eliminated. The tearing will separate the fracture surfaces from contacting to sharp object, eliminating the friction and allow getting the precise value of puncture energy. The theoretical formulation allowing the calculation of the tearing energy associated with this applied prestrain was derived from the theory of Rivlin and Thomas on the rupture of rubber. It was validated with a model extending expressions provided by the linear elastic fracture mechanics (LEFM) to include the non-linear stress-strain behavior of rubber. Finally, the fracture energy in puncture is found greater than that of cutting and smaller than that of tearing as the crack tip diameters are different for various fracture modes (cutting, puncture and tearing).

For practical outcomes, considering the results of puncture by conical and cylindrical probes, since 2005, an alternative method B had been added to F1342 ASTM with 0.5 mm-diameter rounded-tip cylindrical probe. And with the fact that the puncture mechanics by medical needle is different from the puncture by conical and cylindrical probes, a new standard test method ASTM WK 15392 for puncture by medical needles is under development.

LIST OF REFERENCES

1. DANIEL J. HEWETT (1998) *Health Hazard Evaluation Report 97-0068-2690*, Protective Equipment Section, National Institute for Occupational Safety and Health, USA.

2. LESLIE L. F., WOODS J. A., THACKER J. G., MORGAN R. F., MCGREGOR W., EDLICH R.F. (1996) *Needle puncture resistance of medical gloves, finger guards, and glove liners,* Journal of biomedical materials research, vol. 33, n° 1, p. 41 – 46.

3. SALKIN J. A., STUCHIN S. A., KUMMER F. J., REININGER R. (1995) *The effectiveness of cut-proof glove linears : cut and puncture resistance, dexterity, and sensibility,* Orthopedics: thorofare, vol. 18, n° 11, p. 1067 – 1071.

4. STEVENSON A., KAMARUDIN AB MALEK. (1994) *On the puncture mechanics of rubber*, Rubber chemistry and technology, vol. 67, n° 5, p. 743 – 760.

5. MURPHY V. P., KOERNER R. M. (1988) *CBR strength (Puncture) of geosynthetics*, Geotechnical Testing Journal, vol. 3, p. 167-172.

6. NAREJO D., KOERNER R. M., WILSON-FAHMY, R. F. (1996) *Puncture protection of geomembrances, Part II: experimental*, Geosynthetics International, vol. 3, p. 629-653.

7. WILSON-FAHMY R. F., NAREJO D., KOERNER R. M. (1996) *Puncture protection of geomembrances, Part I: theory,* Geosynthetics International, vol. 3, 605-627.

8. TUSHAR K. GHOSH (1998) *Puncture resistance of pre-strained geotextiles and its relation to uniaxial tensile strain at failure*, Geotextiles and geomembrances, vol. 16, p. 293-302.

9. ASTM F 1342 "*Standard Test method for Protective Clothing Material Resistance to Puncture*"(1999) Annual Book of ASTM Standards, vol. 11.03, p. 1102 – 1104.

10. LARA, J., NELISSE, N. CÔTÉ, S., and NELISSE, H. (1992) *Development of a method to evaluate the puncture resistance of protective clothing materials*, Performance of protective clothing: Fourth volume, ASTM STP 1133, James P. McBriarty and Norman W. Henry. Eds. American Society for testing and Materials, Philadelphia, p. 26-37.

11. LARA, J., TURCOT, D., DAIGLE, R. and BOUTIN, J. (1995) *A New Test Method to Evaluate the Cut Resistance of Glove Materials*, Performance of Protective Clothing: Fifth Volume, ASTM STP 1237, James S. Johnson and S. Z. Mansdorf, Eds., American Society for Testing and Materials, Philadelphia.

12. LARA, J., TURCOT, D., DAIGLE, R., and PAYOT, F. (1996) *Comparison of two methods to evaluate the resistance of protective gloves to cutting by sharp blades*, Performance of Protective Clothing : Fifth Volume, ASTM STP 1237, James S. Johnson and S. Z. Mansdorf, Eds., American Society for Testing and Materials.

13. ANTHONY PRIMENTAS (2001) *Puncture and tear of woven fabrics*, Journal of textile and apparel. Technology and management, vol. 1, n° 4, p. 11 – 18.

14. KRISTER FORSBERG & LAWRENCE H. KEITH (1989) *Chemical protective clothing performance,* John Wiley & sons, New York, 307 p.

15. ODIAN GEORGE (1991) *Principles of Polymerization,* 3rd ed., A Wiley-interscience publication, New York, 768 p.

16. SPERLING L. H. (1992) *Introduction to physical polymer science*, 2nd ed., A Wiley-interscience publication, London and New york, 439 p.

17. H. M. JAMES and E. GUTH (1949) *Simple presentation of network theory of rubber, with a discussion of other theories,* Journal of Polymer Science, vol. 4, p. 153 - 181.

18. F. T. WALL (1943) *Statistical thermodynamics of rubber,* Journal of Chemical Physics, vol. 11, p. 527-534.

19. TRELOAR L. R. G. (1975) *The physics of rubber elasticity*, Oxford University Press, London, 310 p.

20. ALAN N. GENT (2001) *Engineering with rubber*, Hanser Publisher,New York,768p.

21. A. KELLY AND N. H. MACMILLAN (1986) *Strong solids,* 3rd ed., Clarendon press, Oxford, 212 p.

22. KINLOCH A. J., YOUNG R. J. (1983) *Fracture behaviour of polymers*, Applied science publishers Ltd, London and New york, 496 p.

23. DAVID K. FELBECK, ANTHONY G. ATKINS (1996) *Strength and Fracture of Engineering Solids*, 2nd ed., Prentice-Hall Inc., 535 p.

24. A. G. THOMAS (1995) *Rupture of Rubber: II. The strain concentration at an Incision*, Journal of Polymer science, vol. 17, p. 177 - 188.

25. BROWN ROGER P. (1996) *Physical testing of rubber*, Chapman & Hall, London and New York, 342p.

26. MCCRUM N. G., BUCKLEY C. P., BUCKNAIL C. B. (1997) *Principles of polymer engineering*, Oxford Science publications, 391 p.

27. POWELL PETER C., HOUSZ A. JAN INGEN (1998) *Engineering with polymers*, 2nd ed., Stanley Thornes (Publishers) Ltd, Cheltenham, 479 p.

28. WITOLD BROSTOW, ROGER D. CORNELIUSSEN (1986) *Failure of plastics*, Hanser Publishers, New York, 486p.

29. HERTZBERG RICHARD W. (1996) *Deformation and fracture mechanics of engineering materials*, 4th ed., John Wiley & Sons Inc., 786 p.

30. ASTM D412 "*Standard Test Methods for Vulcanized Rubber and Thermoplastic Elastomers - Tension*"(1998) Annual Book of ASTM Standards, vol. 09.01.

31. YAMASHITA YOSHIHIRO, KAWABATA SUEO, TAKEUCHI YUJI, SAKAI WATARU (1994) *Biaxial Extension Strength of Carbon Black Reinforced Rubber*, Nihon Gomu Kyokaishi, vol. 67, n° 8, p. 576 – 583.

32. SUEO KAWATABA (1973) *Fracture and mechanical behavior of rubber-like polymers under finite deformation in biaxial stress field,* Journal of Macromolecules Sciences - Physics, vol. 8, p. 605-630.

33. W. H. YANG, K. H. HSU (1971) *Indentation of a circular membrane,* Journal of Applied Mechanics 38, p. 227 - 230.

34. MOONEY M (1940) *A theory of large elastic deformation,* Journal of Applied Physics 11, p. 582-592.

35. RONALD F. GIBSON (1994) *Principles of composite material mechanics*, McGraw-Hill Inc., 678 p.

36. KLAUS FRIEDRICH (1989) *Application of fracture mechanics to composite materials,* Elsevier, 671 p.

37. LAWRENCE J. BROUTMAN, RICHARD H. KROCK (1974) *Composite materials, volume 5: Fracture and fatigue*, Academic Press, New York and London, 465 p.

38. SCHMITZ JOHN V. (1965) *Testing of polymers*, Interscience Publishers, New York, 363 p.

39. ISO 13977: 1999, Protective clothing - Mechanical properties - Determination of resistance to cutting by sharp objects.

40. ASTM D624 "Standard Test Methods for Vulcanized Rubber and Thermoplastic Elastomers - Tearing", Annual Book of ASTM Standards 9.01, USA, 1998.

41. ASTM "*Standard Test procedure for Rubber Property*" (1992) Annual Book of ASTM Standards, vol. 09.01, 878 p.

42. EVARISTO RIANDE ET AL. (2000) *Polymer viscoelasticity: stress and strain in practice*, Marcel Dekker, New York, 879 p.

43. G.R. Tryson, M.T. Takemori, A.F. Yee, Puncture testing of plastics: effects of test geometry, Amer. Soc. Mech. Eng. - AMD 35 (1979) 638 - 647.

44. L.M. Carapellucci, A.F. Yee, Some problems associated with puncture testing of plastics, Poly. Eng. Sci. 27 (1987) 773 - 785.

45. G. S. YEH & D. I. LIVINGSTON (1961) *The indentation and puncture properties of rubber vulcanizates*, Rubber chemistry and technology, vol. 34, p. 937 – 952.

46. S. J. JERRAMS, M. KAYA & K. F. SOON (1998) *The effects of strains rate and harness on the material constants of nitrile rubbers*, Materials and Design, vol. 19, p. 157 – 167.

47. WANG C. & GENT A. N. (1994), *Energy dissipation in cutting and tearing rubber*, IUPAC Polymer Symposium: Functional and High Performance Polymers, Taiwan, p. 629 – 631.

48. KILWON CHO, DAEHO LEE (1998), *Viscoelastic effects in cutting of elastomers by a sharp object*, Journal of Polymer Science Part B: Polymer Physics, Volume: 36, Issue: 8, p. 1283-1291.

49. GENT A. N., LAI S-M., NAH C., WANG C. (1994), *Viscoelastic Effects in Cutting and Tearing Rubber*, Rubber Chemistry and Technology, v. 67, n. 4, p. 610 – 619.

50. Lake, G. J. and Yeoh, O. H., Measurement of rubber cutting resistance in the absence of friction, *Inter. J. Fract.*, v. 14, n. 5, pp. 509-526, 1978.

51. Lake, G. J., and Yeoh, O. H., Effect of crack tip sharpness on the strength of vulcanized rubbers, *J. Polym. Sci.*, 25, p. 1157-1190, 1987.

52. Veith, A. G., A new tear test for rubber, *Rubber Chem. Technol.* 38, p. 700-718, 1965.

53. PETRU BUDRUGEAC (1997) *Accelerated thermal aging of NBR and other materials under air or oxygen pressures,* Die Angewandte Makromolekulare Chemie, vol. 247, p. 19 – 30.

54. P. H. MOTT, C. M. ROLAND (2000) *Aging of natural rubber in air and seawater,* Rubber chemistry and technology, vol. 74, p. 79 – 88.

55. BING FENG JU, KUO-KANG LIU (2002) *Characterizing viscoelastic properties of thin elastomeric membrane*. Mechanics of Materials 34, p. 485 - 491.

56. Nguyen C.T., Vu-Khanh T. and Lara J., Puncture characterization of rubber membranes, Theoretical and Applied Fracture Mechanics 42 (2004) 25 - 33.

57. Nguyen C.T. and Vu-Khanh T., Mechanics and mechanisms of puncture of elastomer membranes, Journal of Materials Science 39, n° 24 (2004) 7361 - 7364.

58. RIVLIN R. S. and THOMAS A. G. (1953), *Rupture of rubber. I. Characteristic energy for tearing,* Journal of Polymer Science, v. 10, n. 3, p. 291 – 318.

59. GREENSMITH H. W. (1963), *Rupture of rubber. X. The change in stored energy on making a small cut in a test piece held in simple extension,* Journal of Applied Polymer Science, v. 7, p. 993 – 1002.

60. VU, T. B. NGA (2005) Thesis: *Mechanics and mechanism of cutting of protective materials,* Université de Sherbrooke, Quebec, Canada.

61. HA ANH, TUNG (2007) Thesis: *Effects of aging on tearing and cutting of rubber,* Université de Sherbrooke, Quebec, Canada.

62. Nguyen C T, Vu-Khanh T, Lara J (2005) A Study on the puncture resistance of rubber materials used in protective clothing. J ASTM Int 2(4):245-258

63. Nguyen C T, Vu-Khanh T, Dolez P I, Lara J (2009) Puncture of elastomers membranes by medical needles. Part I: Mechanisms. Inter J Fract

64. Nguyen C T, Vu-Khanh T, Dolez P I, Lara J (2009) Puncture of elastomers membranes by medical needles. Part II: Mechanics. Inter J Fract

65. Dolez P, Vu-Khanh T, Nguyen C T, Guero G, Gauvin C, Lara J (2008) Influence of medical needle characteristics on the resistance to puncture of protective glove materials. J ASTM Int 5(1):12p